Design Optimization of Variable Stiffness Bi-Stable Composites using Curvilinear Fibers

Luísa Martins Barbosa

Thesis to obtain the Master of Science Degree in

Aerospace Engineering

Supervisor : Prof. Afzal Suleman

Examination Committee

Chairperson:	Prof. Filipe Szolnoky Ramos Pinto Cunha
Supervisor:	Prof. Afzal Suleman
Member of the Committee:	Prof. José Arnaldo Pereira Leite Miranda Guedes

December 2014

Acknowledgments

I would especially like to express my sincere gratitude to my academic supervisor Dr. Afzal Suleman who has been a supportive mentor. Thank you for guiding me in the right directions and for making me challenged my own assumptions.

I would also like to thank my co-supervisor Dr. Ben Nadler for his useful guidance particularly in solving technical issues pertaining to the Finite Elements Analysis aspects of this thesis.

Special thanks are given to Carlos Sousa. The work presented in this thesis owes a great deal to the knowledge passed down by him who provided much technical knowledge and answered my many questions in the early months of my thesis.

I would like to thank the Department of Mechanical Engineering at the University of Victoria for sponsoring my 4-months stay as a visiting graduate student. I appreciate the many learning opportunities that were provided to me.

Last, but definitely not least, I would like to say thanks to my parents and sister for their wise and motivating words. I would not be where I am without their love and support.

Resumo

A possibilidade de explorar as propriedades de rigidez direccionais dos materiais compósitos oferece novas oportunidades de design que podem conduzir a um aumento da performance de laminados biestáveis para aplicações mórficas ou outras aplicações. Nesta tese procura-se analisar os deslocamentos fora do plano de estruturas biestáveis de rigidez variável para que o desempenho destas possa ser maximizado. Esta análise tem importância prática porque permite identificar a deflexão máxima entre estados que uma dada estrutura biestável pode suportar e, assim, perceber se esta é adequada para uma determinada aplicação. A principal novidade do trabalho desenvolvido nesta tese é o desenvolvimento de uma ferramenta para o projecto de laminados biestáveis que tenha em conta os seus dois estados. Para isso considera-se o uso de um algoritmo genético implementado em ModelCenter juntamente com o programa de elementos finitos Abaqus e o Matlab. Foram discutidas duas metodologias de design de laminados com fibras de orientação variável. Uma abordagem que combina as duas metodologias e que assegura a continuidade das fibras ao longo da estrutura foi adoptada. Por fim, foram analisadas duas estruturas com geometrias diferentes (rectangular e trapezoidal) usando duas abordagens distintas. As análises das estruturas óptimas obtidas incluem prever os seus dois estados estáveis bem como as suas características de estabilidade.

Palavras-chave: Laminados biestáveis, Compósitos rigidez variável, Optimização

Abstract

The current study addresses the design of bi-stable variable stiffness composites for morphing aircraft using curvilinear fibers. The design philosophy consists of tailoring out-of-plane displacements using variable stiffness bi-stable laminates in order to optimize the performance of aircraft control surfaces. The study has of practical relevance to the aircraft industry because it enables the performance optimization and thus potentially the reduction of aerodynamic drag and fuel consumption, which is a topic of current interest in the area of greening aircraft.

The main contribution of the present work lies in the development of an optimization framework for bi-stable laminate design based on the integration and coupling of analysis tools (ABAQUS and Matlab) with an optimizer and integrator software (ModelCenter). Two methods to design a variable stiffness laminate are presented in this thesis: a discrete patch design and a continuous design that use a curvilinear function to describe the fiber paths. These two techniques are integrated into a unified design approach that ensures continuity of fiber over the planform of the composite structure and, in doing so, may impart additional structural strength due to the load path continuity. Two different configurations of cantilevered composite laminates geometries (rectangular and trapezoidal) have been studied for illustration and evaluation purposes and the final outcomes include the prediction of the cured shapes and their stability characteristics.

Keywords: Bi-stable laminates design,Variable stiffness composites, Optimization

Contents

List of Tables

List of Figures

Nomenclature

Abbreviations

AFP Automated Fibre Placement

CLT Classical Lamination Theory

DA Darwin Algorithm

FEA Finite Element Analysis

FPM Fibre Placement Machine

NCL Non-Conventional Laminate

OPD Out-of-Plane Displacements

VS Variable Stiffness

List of Symbols

α_i thermal expansions coefficients along each direction

α_1,α_2 thermal expansions coefficients in ply coordinates

α_x,α_y,α_{xy} thermal expansion coefficients in global coordinates

ΔP load increment

ΔT temperature change from cure

κ_x^0,κ_y^0,κ_{xy}^0 curvatures

ν poisson's ratio

$\prod$ total potential energy

σ second Piola-Kirchhoff stress tensor

υ vector of nodal velocities

ε Green-Lagrange strain tensor

ε^T thermal strains

ε_i strains along each direction

ε_x,ε_y,ε_{xy} total strains

ε_x^0,ε_y^0,ε_{xy}^0 midplane strains

A_{ij} components of the in-plane stiffness matrix

B_{ij} components of the bending extension coupling stiffness matrix

c damping factor

D_{ij} components of the bending stiffness matrix

E_{11} longitudinal modulus

E_{22} transverse modulus

f objective function

f vector of body forces

F_v viscous forces

g_m inequality constraints

G_{12} shear modulus

h_p equality constraints

I internal forces

I_a structure's internal forces

M^* artificial mass matrix

$N_{x,y,xy}$,$M_{x,y,xy}$ externally applied forces and moments

$N_{x,y,xy}^T$,$M_{x,y,xy}^T$ thermally induced forces and moments

P external forces

Q_{ij} components of the reduced lamina stiffness matrix

R_a force residual for iteration

T vector of distributed forces acting on the surface

U elastic strain energy

u^0,v^0 in-plane displacements in x and y

V potential energy of forces

w out-of-plane displacement

x design variables of the system

Glossary

Automated fiber placement	an automated manufacturing technology that combines individual tow control found in filament winding machines with compaction and cu-restart capabilities found in a tape laying machines.
Classical lamination theory	is at the basis of laminate stiffness formulation and allows the in-plane stress resultants and moment resultants to be related to the in-plane strains and laminate curvatures via the so called ABD matrices. Classical lamination theory is essentially an extenuation of classical plate theory to composite laminates.
Composite material	are engineered materials made from two or more constituent materials with significantly different physical or chemical properties which remain separate and distinct on a macroscopic level within the finished structure.
Curing	the process of changing the physical properties of a matrix material from a liquid to a solid by chemical reaction by the action of heat and catalysts, alone or in combination, with or without pressure.
Curvilinear fiber paths	a term often used to refer to variable stiffness laminates, highlighthing that the fiber paths are no longer straight.
Fiber angle distribution	used to refer generically to the spatially varying fiber angle orientation of a given ply or laminate within a variable stiffness composite structure.
Laminate	two or more lamina stacked together to form a single material

Lamina	see ply.
Optimization	refers to a process in which the best element or solution is selected from some set of available alternatives. Several methods have been developed to solve optimization problems, the most suitable method is highly dependent on the nature of the problem being solved.
Ply	a single layer of fiber reinforced material within a laminate manufactured by placing sveral repeated courses using a selected course replication strategy.
Stiffness distribution	used to refer generically to the spatially varying stiffness within a variable stiffness composite structure.
Stiffness	used to refer to the overall structural stiffness, in other words how well a given structure is able to resist deformation due to an applied force or moment.
Variable angle tow laminate	an alternative term used to refer to variable stiffness laminates.
Variable stiffness laminate	a laminate within which the fiber orientation angle, and therefore the stiffness properties, vary continuously with spatial location.

Chapter 1

Introduction

1.1 Aims of Research

In order to aid the reader in understanding the key research objectives of this thesis, these are outlined as follows:

- Identify the state of the art on the design of composite bi-stable laminated structures .
- Discuss the potential applications of of bi-stable laminates and provide an understanding into the thermally induced bi-stable behavior.
- Identify and implement an appropriate modelling approach to design variable stiffness bi-stable composite laminates.
- Present an overview on the optimization tools that can be used for the design of variable stiffness composites laminates.
- Develop a design framework that addresses a primary advantage of bi-stable composites: the large achievable deflections between stable states.
- The design framework should consider bi-stable laminates where the laminates are assumed to be a variable stiffness structure to explore the benefits offered by-tow-steering techniques and composite materials while ensuring fiber continuity within the global structure.
- Apply the design framework and formulation to practical applications.

1.2 Literature Review

1.2.1 Aeroespace Morphing and Bistable Composites

In general there is demand from airlines that a new aircraft shows at least a 20% improvement in direct operating costs [1]. Although, a number of system-level improvements can lead to such a reduction in

the direct operating costs, the aircraft industry often considers reducing the structural weight of the aircraft as one of the main options. Researchers have been continuously looking at the means that will help accomplishing this goal.

Thus, recent years have seen a growing interest in conformal shape adaptation, or morphing, as means of significant performance enhancement, particularly in the aerospace domain. This morphing or shape-adaptable structural systems change shape or state in order to change their operating characteristics or as a response to changes in the environmental conditions. Such research offers the potential to create structures which have the advantages of being lighter and simpler than conventional mechanisms as well as enabling geometric changes which would not traditionally be simple to achieve.

Multistable or bistable structures are good candidates to be used as morphing structures because of their ability to remain in natural equilibrium after a shape change occurs without the need for a continuous power supply [2] .

Although multi-stability can be achieved with traditional isotropic materials [3], for morphing aerospace structures, fiber-reinforced laminated composites seem to be better suited because of their superior mechanical properties: high strength and stiffness to weight ratios. Moreover, these laminated composites allow one to design their mechanical properties for a particular application by tailoring their laminate configuration.

Composite materials made of orthotropic layers can develop a residual stress field when subjected to a thermal field that varies with time [4]. The thermal stresses are caused by the mismatch of coefficients of thermal expansion along fiber's directions. If the material is stacked unsymmetrically, residual stresses resulting from differences in coefficients of thermal expansions and elastic properties in each lamina can cause significant out-of-plane displacements. This happens during the curing process of a composite structure when the material is heated up to achieve a desired degree and subsequently cooled down to the room temperature. Figure 1.1 shows the stable states of a cantilevered bi-stable composite.

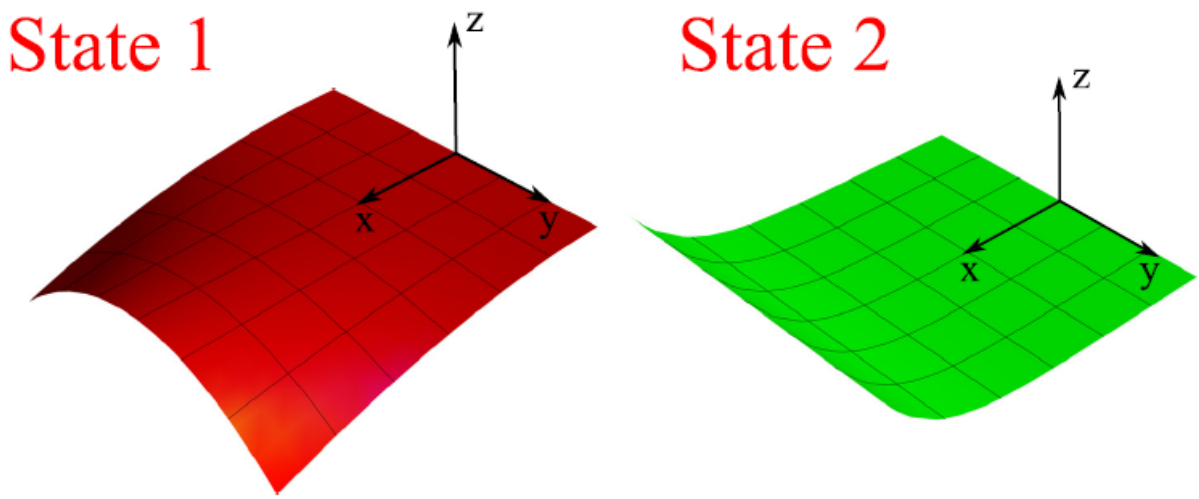

Figure 1.1: Stable shapes of cantilevered bi-stable composites. (Source [5])

Various theoretical and experimental studies have been carried out in order to understand and predict

the behavior of the bi-stable composite structures [6, 7, 8, 9, 10, 11].

For morphing strategies to succeed, the challenge presented by reconciling the inherently conflicting requirements of low mass, shape adaptability, and high load-carrying capacity has to be addressed in the context of a truly integrated multidisciplinary environment [12, 13] .

1.2.2 Tailored Composite Structures

In conventional composite laminate design, the purpose is to find out the material arrangement that best satisfies the posted requirements on, for example, strength, stiffness and cost. The fiber orientation angles are usually chosen from the set $\{0^\circ$,+45° , -45° , 90° $\}$ and remain constant within an entire ply.

Such laminates ignored the full potential of composites because only a limited number of possible combinations of fiber orientation and stacking sequence can be used.

The recent developments introduce the Non-Conventional Laminate concepts (NCLs) that enable the improvement of the mechanical properties and/or weight of the structure. It can be achieved by modifying the stacking sequence within the bounds of conventional design rules and is referred to as laminate tailoring. There are many ways in which laminate tailoring can be achieved, fiber steering will be explored in this thesis.

As in conventional laminates the properties of the composite materials cannot be used to their full extent the concept of laminate tailoring can be taken further by changing the fiber volume fraction in the laminate [14], by dropping or adding plies to the laminate [15], or by using curvilinear fibers ,as shown in Figure 1.2. In this thesis fiber angle variation within a ply will be exploited. This variation in fiber orientation angle result in spatially variable stiffness properties and is therefore referred to as variable stiffness (VS) laminates.

Traditionally, bistable laminates have been developed from prepreg plies stacked together to achieve a layup which is constant over the plan-form of the laminate. However the more recent approach aimed at achieving bistability through variation in layup over the plan-form of the laminate. The laminates having plan-form variation in layup are, in particular, of interest as they offer the prospect of easier integration with the major structure by blending lay-ups across components as discussed by Diaconu et al. [16] and Mattioni and Weaver [17] and Sousa [18]. Such bistable laminates can be manufactured to have curvilinear fibers in a ply using a tow-steering technique to ensure continuity of fibres over the plan-form of the laminates and, in doing so, may impart additional structural strength due to load path continuity.

The concept of variable stiffness composites was first discussed in Hyer and Charette [4] , and Gurdal and Olmedo[19] and is a topic of extensive research activity ever since. Studies have shown improvements in mechanical performance for variable stiffness laminates in comparison to traditional ones

The initial work on variable stiffness composites (Olmedo and Gürdal) showed improvements in the buckling load and axial stiffness for a laminate subject to uniform end shortening. The comparison of a parallel versus a shifted fibre path, used to define a variable stiffness composite, in Waldhart [20] shows that the largest buckling performance increase is found using a shifted fibre path, i.e. using a shifted fibre

path redistributes the loading better, and this gives an increased buckling load for the structure. Fibre steering is used in Li et al. [21] to increase the performance of the bearing strength of bolted holes, and the fibres in this study were steered such that the fibres followed the principle tensile and compressive stress trajectories around the hole. Further, Huang and Haftka [22] have shown that increasing the load carrying capability of a composite plate with a hole in the center and loaded in tension results in a set of nearly concentric circles near the hole where the authors chose to limit the tailored region of the composite with a hole to the region close to the hole. Buckling improvement of a component or structure using a variable stiffness composite has been the topic of several research efforts. The use of a fibre angle variation has been shown, in Gürdal et al. [23] to result in a decoupling of the in-plane stiffness of a composite plate and its buckling performance. A variable stiffness composite panel with the same in-plane properties as a quasi-isotropic composite panel is discussed in Ijsselmuiden et al. [24], and the variable stiffness composite is reported to be able to withstand more than twice the compressive load before buckling occurs compared to a quasi-isotropic composite panel. The paper has allowed for a better understanding of the load redistribution mechanism responsible for an increased buckling load. A buckling load increase of 33.9% with respect to a constant stiffness composite panel is reported in Lopes et al. [25] for a variable stiffness composite panel where overlapping tows are present. Similar results for a clamped square variable stiffness composite panel were reported where an improvement of 66% in the buckling load is found for a simply supported composite panel. The large deflection and stresses of variable stiffness composite laminated (VSCL) plates with curvilinear fibres were studied in [26]. In each ply of these plates, the fibre-orientation angle changes linearly with respect to the horizontal coordinate. In this paper, variable stiffness composite laminated plates with curvilinear fibres were analysed with a new p-version finite element, using third-order shear deformation theory. The authors refers that the curvilinear fibres lead to changes in the stresses, as altering the position of maximum stress at the plate and that these changes in maximum stresses magnitudes and locations may be exploited to improve damage resistance in particular applications. A constant thickness variable stiffness composite cylinder is optimised in Blom et al. [27] to achieve a maximal bending load before buckling occurs, and an improvement of 17% is reported for a variable stiffness composite cylinder with respect to a quasiisotropic composite cylinder of equal weight. The natural frequency of a variable stiffness composite panel is reported in Abdalla et al. [28] to be larger than that of a constant stiffness panel design. The design of variable stiffness conical shells is reported in Blom et al. [29] where the design target was to increase the fundamental frequency of a conical shell using a variable stiffness composite.

This stiffness variation may be discrete, by defining several different patches within a laminate, or continuous, by varying the fiber angle orientation continuously within a ply's domain.

Continuous stiffness variation is essentially a generalization of discrete stiffness variation, which still stems from the more traditional method of defining laminates using a fixed stacking sequence. These two philosophies of design will be discussed later in section 3.1 of this dissertation.

In the context of this thesis, the term variable stiffness laminates refers to the general form of stiffness variation, namely laminates within which the fiber angle in a ply is allowed to vary continuously with

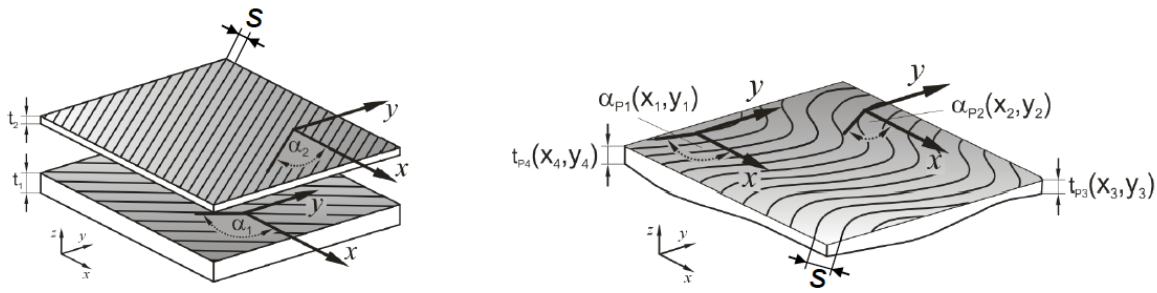

Figure 1.2: Variable stiffness composites (Source [30])

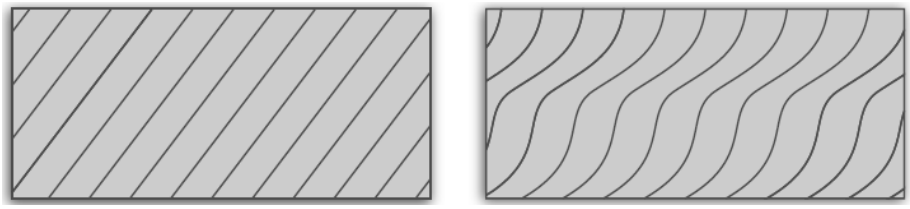

Figure 1.3: Comparing lamina with constant fiber angle (left) and variable fiber angle (right)

spatial location. In the literature these laminates may also be referred to as laminates with curvilinear fiber paths or variable angle tow laminates.

These advanced composite laminates may be manufactured with Tow Placement Technology.

Fiber placement systems have become widely used to manufacture complex aerospace composite structures which resulted in associated reductions in touch labor time, material wastage and part counts [31, 32]. Concurrent research was also performed to design advanced composite structures that have improved structural performance and fabricated using fiber placement. To achieve these performance improvements, tow steering capabilities inherent in the fiber placement machines are typically used to align the composite fibers with the desired structural load paths. Moreover, tow-steering technology enables to locally tailor fiber orientations across the planform of the laminate, giving the designers the opportunity to develop optimum laminates for target applications.

A literature survey on tow placement technology and variable stiffness panels is given in [33].

The original motivation for development of this technology was that the response of fibre-reinforced laminates could be significantly altered by allowing the fibre orientation angle to vary spatially throughout the structure. The potential of VS laminates opens a new branch of research in laminated composite materials; the design complexity requires use of numerical analysis and novel approaches to tackle problems for this type of structural composite laminates.

The basis for improved mechanical performance of composite structures lies in optimized use of the anisotropic properties of the laminate material. The use of traditional laminates with only unidirectional plies poses a strong limitation on the possibilities for laminate design.

As shown above, the increased design freedom and the additional structural strength that results from using a variable stiffness composite has been applied to increase the performance of composite elements in a wide variety of applications. In this work this will be used to optimize and design bi-stable composite laminates.

1.2.3 Design Optimization of laminated Composites

Due to a combination of discrete and continuous design variables composite structures are inherently complex to optimize.

The review of existing literature on optimization of bi-stable laminates demonstrated that existing studies are extremely limited.

Hufenbach [34] considered optimization of bi-stable laminate curvature through a genetic algorithm approach. The objective of the study was to maximize the major curvature in a single stable state, or to meet a specific target curvature. The solution was not guaranteed to be stable and the deflection between two states was not considered.

This study was later extended by Hufenbach and Gude [35] to include failure modes of composite materials as constraints in the optimization, found to be inactive. This work also presented more detailed summary of the ply thickness for maximum curvature. A two-ply example is show in figure 1.4 demonstrating the curvature in a single state with all combinations of relative ply thickness for a $[0/90]_T$ laminate.

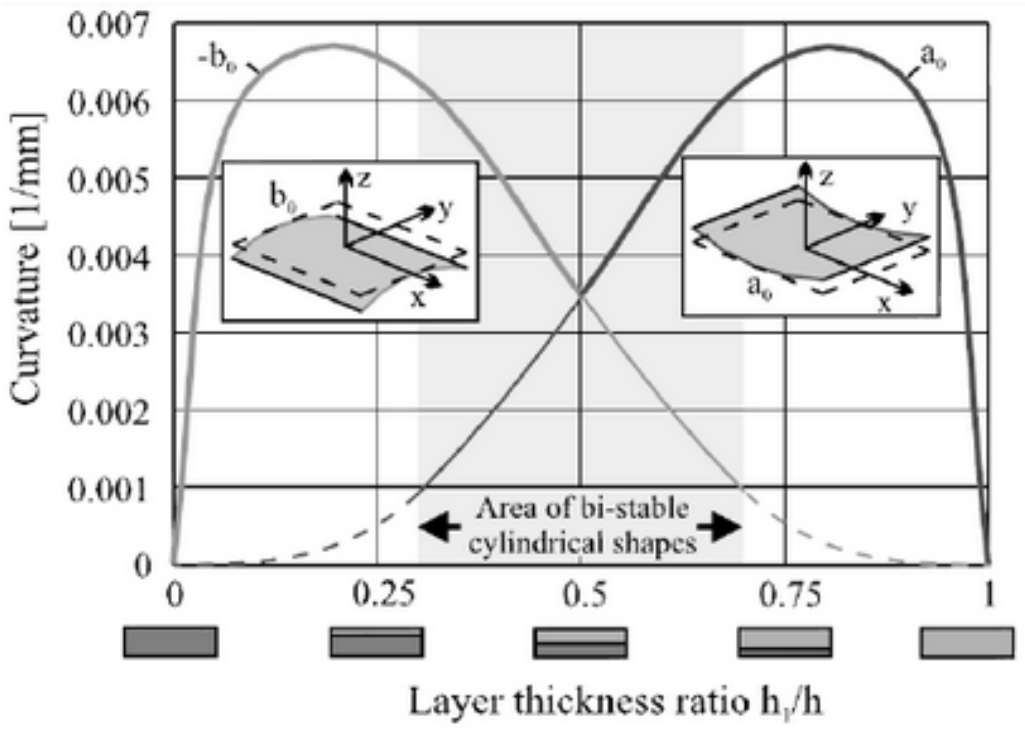

Figure 1.4: Curvature of a two-ply CFRP laminate with variable thickness ratio. Note: laminate size 300 x 300mm, total thisckness h of 1mm, top layer thickness of h_1 (Source [34])

The genetic algorithm was capable of identifying multiple solutions of differing combinations of 0° and 90° plies (variation in number and thickness of plies) to meet a target curvature in a single state within a specified tolerance. Although a primary advantage of bi-stable composites is the large achievable deflection between states, this example highlights the difficult in building an iterative optimization scheme that consider both states.

One a large scale, Panesar and Weaver [36] considered optimization of a blended bi-stable laminate

for a morphing flap application. The design of this structure was limited to discrete ply orientations at 30° intervals. The method used FEA to access the structural deformations and feedback information at each iteration of an ant colony optimization routine. Designs were obtained for both maximize the flap-angle increment and maximum out-of-plane increment.

Variable stiffness bi-stable composites are difficult to design as the optimization problem is no longer limited to a single or several laminates designs but consists essentially of obtained an optimal layup at every point in the structure. Ensuring fiber continuity and laminate manufacturability make difficulties even further. The large number of design variables and constrains associated with variable stiffness design problems make then challenging problems to solve.

An overview of the optimization tools that can be used for the design of variable stiffness composites laminates is provided in [37]. In this paper different parameterization and optimization algorithms are explained and compared and the advantages and shortcomings of each algorithm are discussed.

Due to its robustness and simplicity a Genetic algorithm was implemented, incorporating the feedback from the finite element analysis. The details about the optimization strategy chosen will be discussed later in the section 3.2 of this thesis.

The substantial increase in structural efficiency possible when using variable stiffness laminates and the lack of available design tools motivated the development of a design optimization routine for variable stiffness bi-stable structures.

The obtained solution provides the designer with the fiber angles distribution best satisfying the desired structural performance requirements.

In this work the focus is to find the optimal fibers angles distribution that maximize the relative deflections of the two stable states of a bi-stable composite.

1.3 Thesis Outline

This section summarizes the technical content of each chapter and details the structure of this work to aid the reader in following the information presented in this thesis.

Chapter 1

The literature review gives motivation for the work presented in this thesis by demonstrating the current state of the field, highlighting where new work fits into the existing research and identifying areas of novelty. The review is divided into three main areas: aerospace morphing and bi-stable composites; tailored composite structures; and design optimization of bi-stable composites.

Chapter 2

Chapter 2 deals with the theoretical formulation patented in the the various analyses performed in this work, presenting specific bibliography references, mathematical formulations, the considered assumptions, approximations. This chapter provides much of the necessary background information in order to understand why certain laminates assume two stable states. A brief introduction to the finite

element method and the stability characteristics of multistable composites are also present.

Chapter 3

Several approaches have been developed in order to study variable stiffness laminates. In chapter 3 two representations are explained and the advantages and shortcomings of each approach are discussed. In this chapter are also highlighted the basic concepts of the optimization tool that have been used in the design process of this thesis. The design and computational challenges relate both to the cost of evaluating the function values and the non-convex nature of the design problem. A genetic optimization approach has been used.

Chapter 4

The design of a morphing bi-stable composite using variable stiffness laminates with curvilinear fibers is presented in this thesis. The framework that was developed to create such a design is presented in chapter 4. This chapter is divided in four sub-sections: Laminate Modeling Philosophy; Tow-steering Compatibility Constraint; Design Objective and Design Framework Implementation.

Chapter 5

In chapter 5 the framework developed were applied for two candidate designs in order to validate the use of a maximum deflection based objective function in the design of a morphing bi-stable laminate. The first model is referred to as rectangular laminate and the second one as trapezoidal laminate. Three different analyses were considered: one, a parametric study with only unidirectional fibers; two, a preliminary study that considers a less complex structure which could easily be tested within a short timespan; and three, a final study. The bistable equilibrium configurations developed and investigated in the present research could be used as an efficient structure for morphing wings.

Chapter 6

Finally, chapter 6 summarizes the main conclusions of this work and highlights the novel findings which are of interest in the field of morphing laminate structures. Specifically the success of the presented work with reference to the key objectives outlined in Section 1.1 is discussed. This section also includes discussion on a number of potential paths for future work.

Chapter 2

Structural Theory

In order to understand why certain laminates assume two stable states an overview of governing equations is presented. A brief introduction to the finite element method and the stability characteristics of multistable composites are also present in this chapter.

2.1 A short introduction to composites

A composite material, as the name suggests, is a material system which consists of two or more phases on a macroscopic scale. The constituents will generally have significantly different physical or chemical properties and are combined to create a material with properties superior to those of its constituents. The different phases in a typical composite material are shown in figure 2.1.

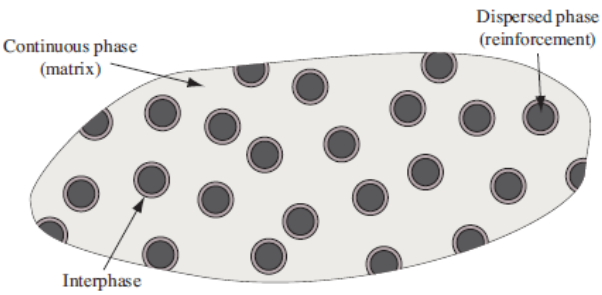

Figure 2.1: Phases of a composite material

Traditional composites are usually constructed of a fibrous material with high strength and stiffness properties embedded in a resin matrix. The configuration and volume ratios of the two constituents determine the stiffness and strength behavior of the resulting material. For instance, a typical composite material used in the aerospace industry is graphite-epoxy, which contains graphite fibers laid parallel to one another and held in place by an epoxy matrix material. This produces an orthotropic material (one with different stiffness and strength characteristics in orthogonal directions) with higher strength and stiffness properties per unit weight than corresponding isotropic materials (such as aluminum). Stiffness properties in fiber direction (E_1) are usually an order of magnitude larger than in the transverse direction (E_2). Strength properties of unidirectional lamina depend both on fiber orientation and load direction.

The most practical application of these composite materials was found to be in the form of laminates (see figure 2.2), in which a structure is constructed of many layers (laminae) of these directional materials and defined by the ordered layup, or stacking sequence, of its individual plies.

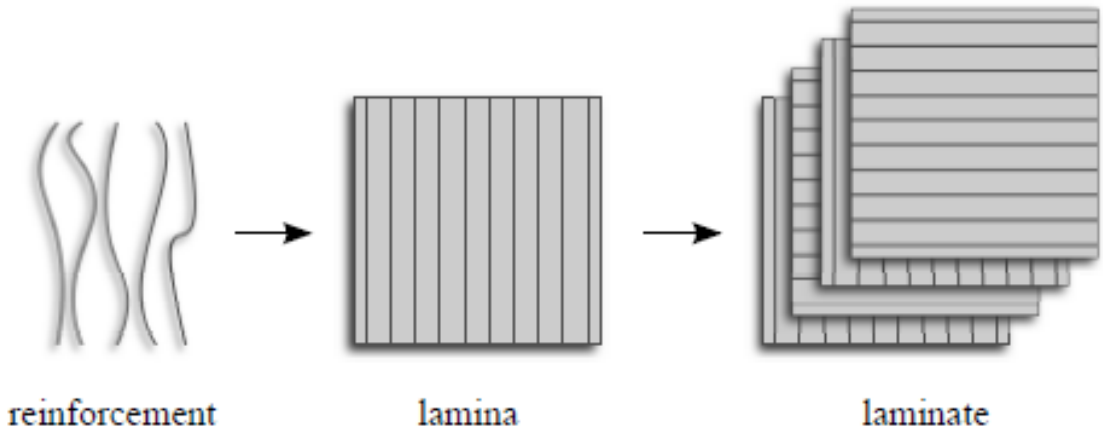

Figure 2.2: From reinforcement to laminate

Using these composite materials, the potential for stiffness variation increased tremendously, for besides the possibilities of thickness changes due to changing the number of plies throughout the structure, there also existed manufacturing variability with respect to material ratio (volume fractions), fiber spacing and fiber orientation, not to mention unintentional variations of the material properties by way of voids and imperfections within the composite material.

Interested readers are referred to text books such as Tsai and Hahn [38] or Kassapoglou [39] for additional information about composites and composite design.

2.2 Multistable Composites

Multistability can be imparted into fibre-reinforced composites by utilising the residual stresses developed during cool-down.

Unsymmetric laminates that are cured at an elevated temperature deform severely as they are cooled to their service temperature. Under certain conditions the thermal warping can lead to two stable states. These deformations are due to the mismatch in the coefficients of thermal expansion α_i along different fibers directions. This means that when a composite material made of orthotropic layers is subjected to a temperature difference, it will experience different strains ε_i along each direction i :

$$\varepsilon_i = \alpha_i \times \Delta T \tag{2.1}$$

Thus, when the laminate is cooling down from the autoclave cure temperature to a service temperature, say, room temperature, the layers with different orientation angles will tend to have different strains. As the layers cannot freely stretch relative to each other, the laminate will develop a curvature that best

accommodates the conflicting individual strains and that minimizes the residual stresses associated with the inability of each layer to stretch by the amount given by equation 2.1.

As the temperature change relative to the curing temperature increases, the magnitude of the laminate's curvature also increases. If the temperature change exceeds a certain threshold there is no curvature of the laminate that can accommodate the conflicting thermal strains of the various layers. In that case, the influence of one of these conflicting thermal strains prevails and the laminate acquires a curvature dominated by the thermal strains of one of the layers. However, significant residual stresses will be present and if an appropriate load, referred to as the snap-through force, is applied it will acquire a curvature dominated by the thermal strains of those other layers.

Figure 2.3 shows this behaviour for an example square $[0/90]_T$ laminate.

For a low ratio of edge length to thickness only a single stable state is observed, point A, with x- and y-curvatures of equal magnitude in opposite out-of-plane directions. As the ratio increases the solution bifurcates, point B. Beyond this point two approximately cylindrical stable states are observed, points C and D, while the saddle state becomes unstable (dashed line).

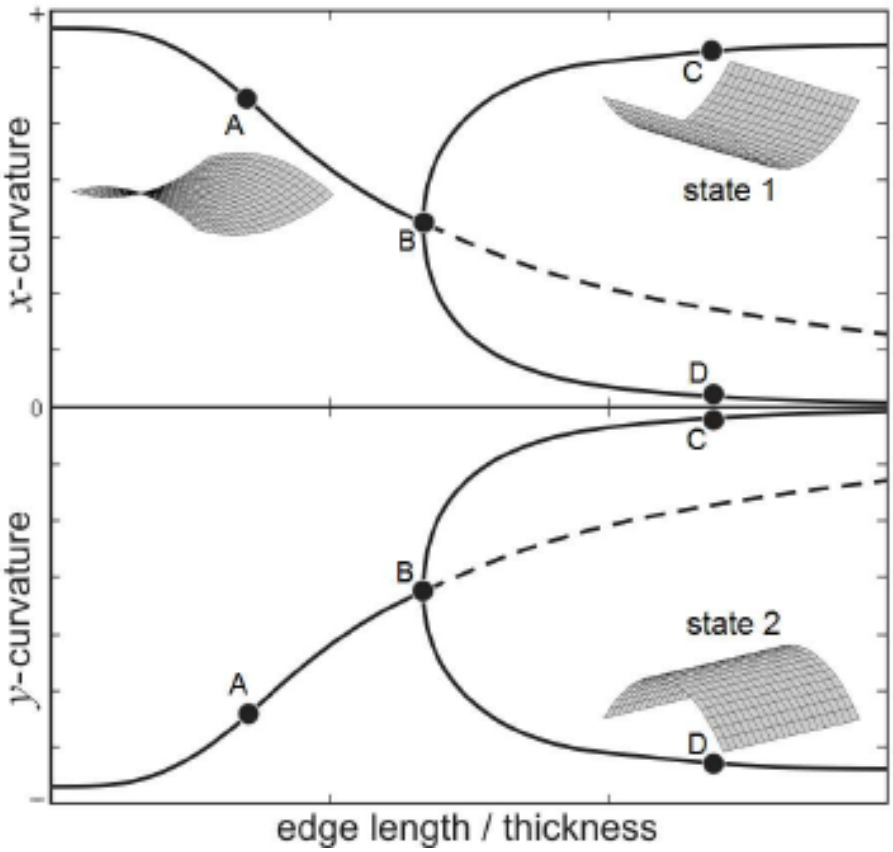

Figure 2.3: Stable (solid) and unstable (dashed) shapes of a $[0/90]_T$ laminate (Source [7])

The possibility of snapping (bifurcating) from one configuration to another by means of an actuation system expands the range of possible application of these type of structures as the actuator is only required to provide energy during the snap-though process and not to maintain a configuration since both are stable (Mattioni et al.,2005, 2006 [40, 41]).

2.2.1 Nonlinear extension to Classical Laminated Plate Theory

A stack of layers of different materials, with different fiber orientations and in which its planar dimensions is some orders of magnitude larger than its thickness is, by definition, a laminated composite.

The understanding of behavior and response of these materials to different boundary conditions and forces is well defined by Classical Laminated Plate Theory (CLPT). This theory is an extension of Classical Plate Theory to composite laminates and is based on a number of assumptions:

1. Displacements are continuous throughout the laminate.
2. Kirchhoff hypothesis is valid.
3. Strain-displacement relationships are linear.
4. Material is linear elastic.
5. Through-thickness stresses are small in comparison to in-plane stresses.

These assumptions are important for simplification of mathematical models that represents laminates. For more detailed description, please refer to [42, 43].

This theory smears the properties of the individual lamina to give overall laminate properties defined by the in-plane (A), coupling (B) and flexural (D) stiffness matrices.

While CLT is capable of accurately predicting static deformations, natural vibration, frequencies and mode shapes, buckling loads and mode shapes, and thermal expansion properties, there are cases where the theory fails to capture the correct behaviour. One situation in which CLT fails to predict the physical reality was observed by Hyer [6]. CLT predicts all asymmetric laminates to have a single stable state of anticlastic or 'saddle' curvature. Hyer [6] documented the room-temperature shapes of a number of thin asymmetric laminates and found that some exhibit approximately cylindrical shape. Furthermore, in some cases two stable states of opposing cylindrical curvature were observed. This contrast to the predictions of CLT was observed for a four-ply $[0_2/90_2]_T$ laminate. However, when the thickness of the laminate was doubled to $[0_4/90_4]_T$, the observed shapes conformed to the theoretical predictions.

In fact, given that the out-of-plane displacements observed in bi-stable composites are many laminate thicknesses in magnitude, geometric nonlinearity must be considered in the analysis.

The constitutive equations, in terms of the force and moment resultants, are given by:

$$\begin{bmatrix} N_x \\ N_y \\ N_{xy} \\ M_x \\ M_y \\ M_{xy} \end{bmatrix} = \begin{bmatrix} A_{11} & A_{12} & A_{16} & B_{11} & B_{12} & B_{16} \\ A_{12} & A_{22} & A_{26} & B_{12} & B_{22} & B_{26} \\ A_{16} & A_{26} & A_{66} & B_{16} & B_{26} & B_{66} \\ B_{11} & B_{12} & B_{16} & D_{11} & D_{12} & D_{16} \\ B_{12} & B_{22} & B_{26} & D_{12} & D_{22} & D_{26} \\ B_{16} & B_{26} & B_{66} & D_{16} & D_{26} & D_{66} \end{bmatrix} \begin{bmatrix} {\varepsilon_x}^\circ \\ {\varepsilon_y}^\circ \\ {\gamma_{xy}}^\circ \\ {\kappa_x}^\circ \\ {\kappa_y}^\circ \\ {\kappa_{xy}}^\circ \end{bmatrix} - \begin{bmatrix} {N_x}^D \\ {N_y}^D \\ {N_{xy}}^D \\ {M_x}^D \\ {M_y}^D \\ {M_{xy}}^D \end{bmatrix} \tag{2.2}$$

where the Ns and Ms are the force and moment resultants; the As, Bs, and Ds are the components of the ABD matrix; the ε° and κ° are the midplane strains and curvatures; and the N^Ds and M^Ds

are effective force and moment resultants. The strains are given by the simplified nonlinear strain-displacement relations for small strains and moderate rotations:

$$\varepsilon_x{}^\circ = \frac{\partial u^\circ}{\partial x} + \frac{1}{2}(\frac{\partial w^\circ}{\partial x})^2 \tag{2.3a}$$

$$\varepsilon_y{}^\circ = \frac{\partial v^\circ}{\partial y} + \frac{1}{2}(\frac{\partial w^\circ}{\partial y})^2 \tag{2.3b}$$

$$\gamma_{xy}{}^\circ = \frac{\partial u^\circ}{\partial x} + \frac{\partial v^\circ}{\partial y} + (\frac{\partial w^\circ}{\partial x})(\frac{\partial w^\circ}{\partial y}) \tag{2.3c}$$

where u° , v° , and are the midplane displacements in the x, y, and z directions, respectively.

The terms involving w° are the nonlinear terms. The equations for the curvatures in terms of the displacements are

$$\kappa_x{}^\circ = -\frac{\partial^2 w^\circ}{\partial x^2} \tag{2.4a}$$

$$\kappa_y{}^\circ = -\frac{\partial^2 w^\circ}{\partial y^2} \tag{2.4b}$$

$$\kappa_{xy}{}^\circ = -2\frac{\partial^2 w^\circ}{\partial x \partial y} \tag{2.4c}$$

The effective force and moment resultants take into account strain effects are defined as

$$N_x{}^D \equiv \int_{\frac{H}{2}}^{-\frac{H}{2}} (\varepsilon_x^D \overline{Q_{11}} + \varepsilon_y^D \overline{Q_{12}} + \gamma_{xy}^D \overline{Q_{16}}) dz \tag{2.5a}$$

$$N_y{}^D \equiv \int_{\frac{H}{2}}^{-\frac{H}{2}} (\varepsilon_x^D \overline{Q_{12}} + \varepsilon_y^D \overline{Q_{22}} + \gamma_{xy}^D \overline{Q_{26}}) dz \tag{2.5b}$$

$$N_{xy}{}^D \equiv \int_{\frac{H}{2}}^{-\frac{H}{2}} (\varepsilon_x^D \overline{Q_{16}} + \varepsilon_y^D \overline{Q_{26}} + \gamma_{xy}^D \overline{Q_{66}}) dz \tag{2.5c}$$

$$M_x{}^D \equiv \int_{\frac{H}{2}}^{-\frac{H}{2}} (\varepsilon_x^D \overline{Q_{11}} + \varepsilon_y^D \overline{Q_{12}} + \gamma_{xy}^D \overline{Q_{16}}) z dz \tag{2.5d}$$

$$M_y{}^D \equiv \int_{\frac{H}{2}}^{-\frac{H}{2}} (\varepsilon_x^D \overline{Q_{12}} + \varepsilon_y^D \overline{Q_{22}} + \gamma_{xy}^D \overline{Q_{26}}) z dz \tag{2.5e}$$

$$M_{xy}{}^D \equiv \int_{\frac{H}{2}}^{-\frac{H}{2}} (\varepsilon_x^D \overline{Q_{16}} + \varepsilon_y^D \overline{Q_{26}} + \gamma_{xy}^D \overline{Q_{66}}) z dz \tag{2.5f}$$

where H is the laminate thickness and the $\overline{Q}$s are the transformed reduced stiffnesses. The ε^Ds and the γ^Ds are effective strains, take into account thermal effects, and are defined as

$$\varepsilon_x^D \equiv \varepsilon_x^T \tag{2.6a}$$

$$\varepsilon_y^D \equiv \varepsilon_y^T \tag{2.6b}$$

$$\gamma_{xy}^D \equiv \gamma_{xy}^T \tag{2.6c}$$

The superscript “T” represents thermally-induced strain effects. The strains caused by temperature change are given by

$$\varepsilon_x^T = \alpha_x \Delta T \tag{2.7a}$$

$$\varepsilon_y^T = \alpha_y \Delta T \tag{2.7b}$$

$$\gamma_{xy}^T = \alpha_{xy} \Delta T \tag{2.7c}$$

where

$$\alpha_x = \alpha_1 \cos^2\theta + \alpha_2 \sin^2\theta \tag{2.8a}$$

$$\alpha_y = \alpha_1 \sin^2\theta + \alpha_2 \cos^2\theta \tag{2.8b}$$

$$\alpha_{xy} = 2(\alpha_1 - \alpha_2)\cos\theta\sin\theta \tag{2.8c}$$

and θ is the fiber angle relative to the x axis. The quantities α_1 and α_2 are the thermal expansion coefficients in the principal material coordinate system, and ΔT is the change in temperature from the cure temperature.

2.2.2 The Principle of Minimum Total Potential Energy

The Principle of Minimum Total Potential Energy states that the total potential energy, $\prod$, is the sum of elastic strain energy, U, stored in the deformed body and the potential energy, V , of forces.

$$\delta \prod = \delta(U + V) = 0 \tag{2.9}$$

The relation above is the basis of this principle and can be easily obtained having in attention the principle of virtual displacements:

$$\int_V (\delta\varepsilon^T \sigma - \delta u^T f) dV - \int_S \delta u^T T dS = 0 \tag{2.10}$$

where the variables stand for:

u vector of displacements

T vector of distributed forces acting on the surface

f vector of body forces

σ associated second Piola-Kirchhoff stress tensor
ε Green-Lagrange strain tensor

When external forces are conservative, the change in potential energy of forces is

$$V = -\int_S u^T T dS - \int_V u^T f dV \tag{2.11}$$

and the change of elastic strain energy U due to infinitesimal variations is

$$U = \int_V \delta\varepsilon^T \sigma dV \tag{2.12}$$

Replacing these two expressions on 2.10 leads to 2.9.

The multiple stable shapes, which appear when the structure is subjected to thermal loads can be determined by minimizing the total potential energy of the structure. Based on this approach, many analytical solutions were proposed for analyzing the bi-stable shapes of simple rectangular plates, the interested reader is referred to [7],[4],[44],[45],[46]. However, for complex structures it is necessary to employ complex nonlinear FEA in order to determine the bi-stable or multi-stable shapes and to study the snap-through from one shape to another.

2.3 Analysis Background and FE Modeling

Most of the developed analytical solutions to predict the cured shape of unsymmetric composites are based on using Rayleigh-Ritz minimization of the total potential energy in conjunction with polynomial approximations of the displacements or of the mid-plane strains. These models can only be used for simply geometries which make the Finite Element Analysis (FEA) better suited for predicting the behavior of bi-stable or multi-stable structures with more complex geometries and boundary conditions.

Moreover, since individual properties can be defined per element, this approach is also well suited to studying variable stiffness structures.

Finite element modelling is an ubiquitous, well tested tool for the analysis of mechanical components and can easily be integrated in a design optimization procedure.

Due to the intrinsic nonlinearity of the snap-through phenomenon in bi-stable structures the finite element code have to be carefully coaxed in order to predict behavior for each particular concept [16]. ABAQUS finite element commercial software was selected for the current study. This software provides varying orders of element formulation and offers flexibility to handle intricate details suitable to a range of applications.

In this section the theoretical background of FEA methodology is present.

2.3.1 Solution of nonlinear system of equations

As previously said, a nonlinear system of equations is required to be solved in large deformation analysis of bi-stable or multi-stable composite structures.

For this analysis the most important part of the manufacture is the cool-down after the curing process which is when the residual stresses are built in to the laminate. The asymmetric thermal expansion is the main cause for the stress generation and the stability characteristics of the plate are entirely defined once the temperature reaches the room value.

For the purpose of this thesis, viscoelastic effects and moisture absorption will be neglected during the analysis.

The common methods of solving these nonlinear systems of equations are found by specifying the loading as a function of time and incrementing time to obtain the nonlinear response. Therefore ABAQUS breaks the simulation into a number of time increments and finds the approximate equilibrium configuration at the end of each time increment [47].

In a finite element analysis, for a body to be in equilibrium, the net force at every node must be zero. The internal loads acting on a node are caused by the stresses in the elements that are attached to that node. (see figure 2.4)

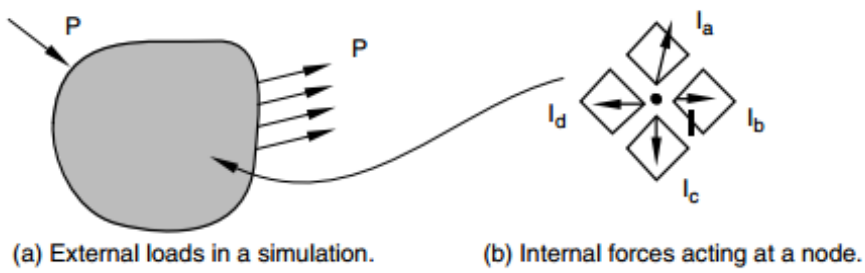

Figure 2.4: Internal and external loads on a body (Reproduced from [47])

Therefore, the basis statement of equilibrium is that the internal forces,I, and the external forces, P, must balance each other:

$$P - I = 0 \tag{2.13}$$

The nonlinear response of a structure to a small load increment, ΔP, is shown in figure 2.5.

ABAQUS uses the structure's tangent stiffness, K_0, which is based on its configuration at u_0, and ΔP to calculate a displacement correction c_a, for the structure. Using c_a the structure's configuration is updated to u_a.

Then, ABAQUS calculates the structure's internal forces, I_a, in this updated configuration. The difference between the total applied load, P, and I_a can now be calculated as,

$$R_a = P - I_a \tag{2.14}$$

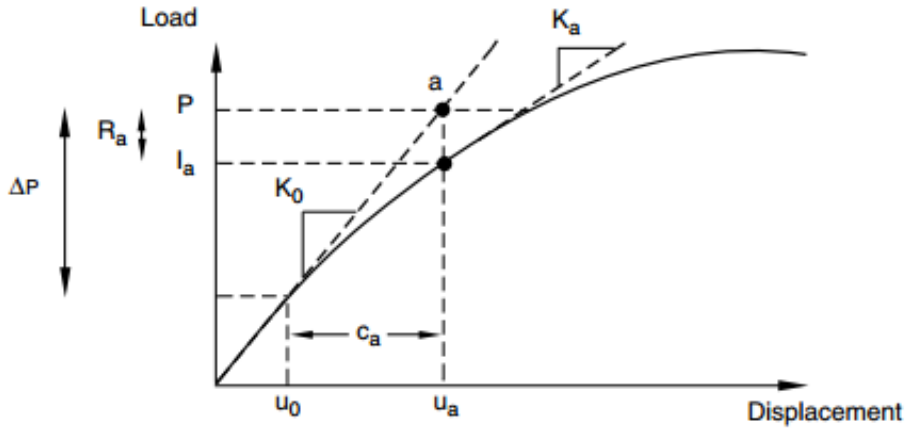

Figure 2.5: First iteration in an increment (Reproduced from [47])

where R_a is the force residual for the iteration.

If R_a is zero at every degree of freedom in the model, point a in figur 2.5 would lie on the load-deflection curve and the structure would be in equilibrium. In a nonlinear problem R_a will never be exactly zero, so ABAQUS compares it to a tolerance value. If R_a is less than this force residual tolerance at all nodes ABAQUS accepts the solution as being in equilibrium.

If R_a is less than the current tolerance value, P and I_a are considered to be in equilibrium and u_a is a valid equilibrium configuration to the structure under the applied load.

Before ABAQUS accept the solution, it also checks that the last displacement correction, c_a, is small relative to the total increment displacement $\Delta u_a = u_a - u_0$. If c_a is greater than a fraction of the incremental displacement ABAQUS performs another iteration. Both convergence checks must be satisfied before a solution is said to be converged for that time increment. For more details on convergence criteria for nonlinear problems in ABAQUS please see [47]

For each iteration in a nonlinear analysis ABAQUS forms the model's stiffness matrix and solves a system of equations.

If the structure is in a state of equilibrium K is positive definite (all its eigenvalues are real and positive) whereas it is non-positive definite if the structure is in a state of unstable equilibrium (at least one negative eigenvalue).

If a negative eigenvalue is found during the numerical simulation it means that the solution jumped after a singular point and found an unstable equilibrium configuration. This does not necessarily affect the accuracy of the solution. It only means that between two successive increments there exists a configuration for which the tangent stiffness matrix is singular, a condition typical of limit point and bifurcation points.

These unstable post-buckling analysis usually pose convergence difficulties and therefore require the application of special nonlinear tecniques. There are various strategies for dealing with this issue. For snap-through problems an explicit dynamic analysis is the most reliable because it accounts for the inertial effects but can be very expensive from the computational view and require a detailed description

of the damping characteristics of the structure.

Mattioni et al. [48] presents a pseudo-dynamic solution strategy to address the complexity of the snap-through process. They proposed the use of a static analysis that includes viscous forces to damp local instabilities when convergence is difficult to achieve and showed that by doing so a dynamic analysis can be avoided. They make use of Abaqus/Standard option to stabilize the problem by including automatic stabilization in any nonlinear quasi-static procedure. Viscous forces of the form

$$F_v = cM * v \tag{2.15}$$

are added to the global equilibrium equations.

$$P - I - F_v = 0 \tag{2.16}$$

where $M*$ is an artificial mass matrix calculated with unit density, c is a damping factor, v is the vector of nodal velocities. Using this solution strategy it is possible to converge to either of the equilibrium states by simply modifying the amount of artificial damping used. It is important to note that with the pseudo-dynamic scheme the equilibrium configuration can be affected by the amount of damping and to ensure accuracy it is important to choose c as the smallest value that suppresses the local instabilities. For more detailed description, please refer to [48, 47].

2.4 Stability Characteristics / Snap-Through Analysis

To be able to actuate bi-stable plates, that is, to snap the plates from one stable state to another, it is necessary to apply some actuation loads on the plates. Such loads can be applied using shape memory alloys [49, 50], piezoelectric patches [2, 51] or concentrate loads applied transversally on various locations on the plate.

In order to perform the snap-through analysis, some concentrate loads were applied on the plate. The aim of this analysis is to compute the maximum out-of-plane load that the optimum laminates can withstand before changing configuration.

ABAQUS FEA methodology was used to investigate the stability characteristics of the optimum unsymmetric laminates studied in this work.

This can be attained by utilizing a nonlinear step(s) similar to the methodology for obtaining the room temperature shapes of the laminate.

The analysis is carried out using the following five steps approach:

1. In the first step residual stresses are introduced by cooling it to the room temperature.

2. Actuation loads are applied on the structure to make the laminate deform in one of the stable shape of the laminate. The applied load is normally higher than the one that cause the panel to snap-through. This nonlinear step is used to predict the load-deflection curve.

3. The loads are removed to acquire the first stable shape.

4. Actuation loads are now applied in the opposite direction to make the structure to snap-through and deform towards the possible second stable shape. The applied load is normally higher than the critical value. Load deflection curve can be predicted in this nonlinear analysis step.

5. These loads are removed to observe a possible second stable shape.

During the application of the load, the structure will first deform elastically, when the force reaches a critical magnitude, the structure will buckle and eventually rest in the other stable configuration once the load is removed.

This geometric snap-buckling instability is one of the most difficult tasks involved in the buckling phenomenon. The snap-through instability describes a trasition between two non-local stability states. Euler buckling represents a globally stable catastrofe and is attributed to the loss of stability where the post-critical state is infinitesimaly close to the pre-critical state. Snap-through, on the other hand, refers to a globally unstable catastrophe, known as a dual cusp catastrophe, where the pre- and post-critical states are separated by some finite distance. Once the critical criteria for stability loss is met; there are no stable, intermediate states, and a jump between states occurs.

From the static point of view this problem represents an unstable collapse, than when applying a concentrate load to trigger snap-through behavior the laminate may run into local instabilities. The thinner the laminate the higher the possibility of local instabilities to occur. A stactic, stabiize step was then performed, Tawfik et al. [52].

Chapter 3

Variable Stiffness Laminate Modelling and Design

3.1 Modeling Variable Stiffness Laminates

Variables stiffness laminates are laminates within which stiffness properties are a function of spatial location, in other words stiffness properties change point to point. This stiffness variation may be discrete, by defining several different patches within a laminate, or continuous, by varying the fiber angle orientation continuously within a ply's domain.

The figure below shows schematic examples of both discrete and continuous variable stiffness laminates.

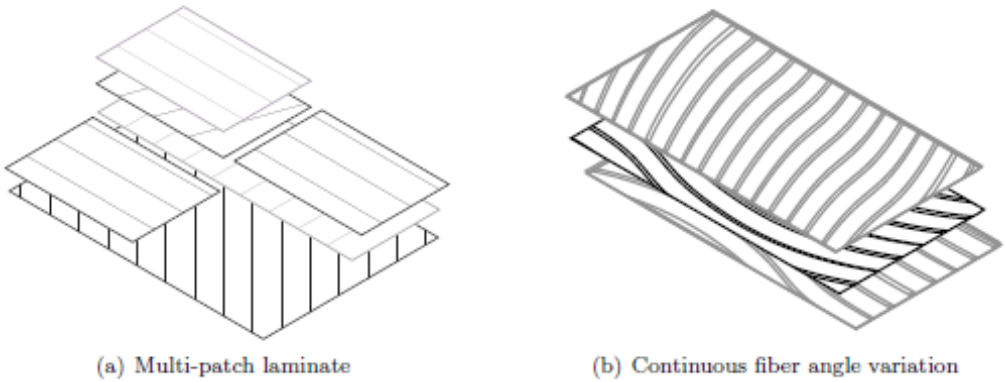

Figure 3.1: Schematic representation of two variable stiffness laminates. The first is achieved by defining several different constante stiffness patches within a single laminate and the second consisting of one or more plies with countinuouly varying fiber angle orientation

Superior structural performance of variable stiffness design vs constant stiffness design have been demonstrated for different properties such as buckling capacity [53, 24, 54], elastic behavior [19], stiffness [55], compressive buckling and first-ply-failure [25], maximum frequency [29] and post-buckling progressive damage [56].

In this section is provided a broad overview of methods currently available to model and design optimization of variable stiffness laminates.

Several approaches have been developed in order to study variable stiffness laminates. Roughly, it is possible to classify these approaches in three different representations: one, discrete stiffness representation; two, direct stiffness modeling and three, using a functional representation of the fiber paths. The direct stiffness modeling is beyond the interest of this thesis and therefore will not be addressed here.

3.1.1 Discrete Stiffness Representation

The discrete fiber representation is the most commonly used method for defining stiffness variation within a structure. This representation is also referred to as Patch design. A ”patch” defines a region within the structure where the lamination sequence is uniforme. Figure 3.2 shows an extension of a multi-patch laminate of figure 3.1, to a level where the laminate is defined locally at each point in the structure. The result is a fiber angle defined at specific points within a discretized structure.

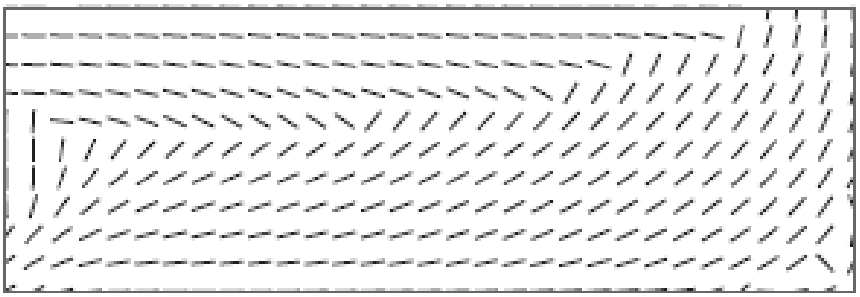

Figure 3.2: Example of discrete fiber angle distribution (Source Setoodeh et al. [55])

A drawback of this method is the difficulty of ensure fiber angle continuity between adjacent elements.

3.1.2 Functional Fiber Path Representation

These representative methods make use of mathematical functions to define the fiber angle variation along the laminate.

The curvilinear function is identified by a set a parameters in a pre-defined mathematical expression [57] or by interpolating a pre-defined function to prescribed key points [22].

All these methods have the advantage of ensuring fiber path continuity, however, the scope of the number of design variables, and therefore the scope of the solution, is often limiting.

The first authors that introduce a fiber path parameterization scheme were Olmedo and Gurdal (1993) [58]. They define the fiber angles as varying linearly along either the x or y axis and demonstrate buckling load improvements up to 80% with respect to the best straight fiber designs.

Years later, Tatting and Gurdal [23] generalize the path definition formulation to vary linearly along an arbitrarily defined axis, x', such that the fiber angle, $\theta(x')$, is defined as,

$$\theta(x') = \phi + (T_1 - T_0)\frac{\mid x' \mid}{d} + T_0 \tag{3.1}$$

where T_0 and T_1 are the fiber angles at the beginning and the end of the characteristic length,d. The orientation of x' with respect to the global x-axis is defined by the angle ϕ.

The terms of the equation 3.1 are represented graphically in figure 3.3. They also introduce a compact notation such that plies with linear variation can be denoted as $\phi < T_0, T_1 >$.

The concept of continuously varying the angle of the fiber path making use of a mathematical function has been the subject of through investigation. The interested reader is referred to [59, 27, 60, 29, 61, 62] for further information.

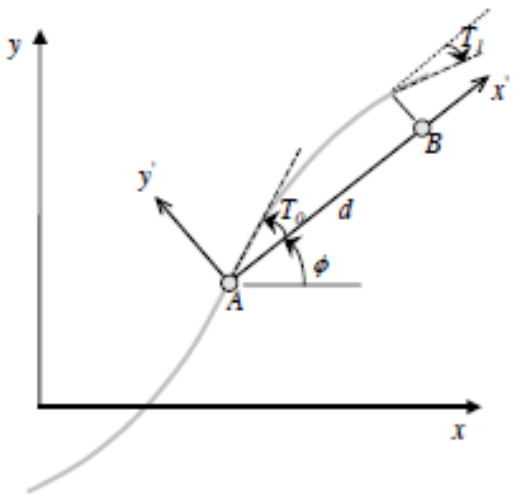

Figure 3.3: Schematic representation of a fiber path defined using linear variation which can be compactly denoted as $\phi < T_0, T_1 >$ and where d represents a predifined length over which the variation occurs (Reproduced from Gurdal et al. [23])

3.2 Design Variable Stiffness Laminates

The numerical method presented in sections 2.3 and 2.4 of chapter 2 has dealt exclusively with the numerical solution of the problem. This analysis provides the structural response of a given laminate, which can be translated into a suitable 'performance' with regards to the application of the structure. However, the numerical analysis has no ability to recommend possible laminate designs or to calculate the sensitivity of response with respect to some design parameter, such as a dimension or the laminate stacking sequence.

An automated process, called design optimization, is subsequently used to determine the best values of certain design parameters so that the performance of the structure is maximized. These aspects of the design process are governed by optimization techniques.

As said before, the FE structural analysis of this thesis will be accomplished using Abaqus software that will be iteratively run through Phoenix Integration's ModelCenter optimization tool. Phoenix Integra-

tion Inc. is a leader in the design process optimization software market and has had a big impact on the aerospace engineering community; as reported by NASA in [63].

The solution of a standard optimization problem can be expressed as:

$$\begin{aligned} \text{minimize} \quad & f(\mathbf{x}) \\ \text{by varying} \quad & \mathbf{x} \in \mathbb{R}^n \,, \\ \text{subject to} \quad & h_p(x) = 0, \quad p = 1, 2, ..., N_p \\ & g_m(x) \geq 0, \quad m = 1, 2, ..., N_g \end{aligned} \tag{3.2}$$

The vector x represents the design variables of the system, while f is defined as the objective function and h_p and g_m are the equality and inequality constraints, respectively. Note that the maximization of f is equivalent to the minimization of $-f$. The design variables may be either infinitely-valued, which implies continuity throughout the real numbers, or discrete-valued, for which only certain values of the variables are permitted.

Examples of discrete variables include ply thicknesses and orientation angles, which may be limited due to manufacturing constraints, and integers representing the number of stiffeners included in the structure. The inequality and equality constraints divide the domain into a feasible and infeasible design space, and the correct solution of the optimization problem results in a vector x which generate the minimum/maximum value of f while still being located within this feasible design space.

For nonlinear objective functions, many local optima may exist which still satisfy all the expressions of equation 3.2. However, the goal of the optimization process is to find the actual global optimum which achieves the best performance when compared to all other feasible designs. For most optimization techniques, this assurance of global optimality can never be proven, though some techniques (most notably genetic algorithms) strive to attain this demand.

The ease, or difficulty, with which problem 3.2 can be solved and the range of algorithms that can be used to solve it depend primarily on analysis complexity, model complexity and optimization complexity.

In fact, the more complicated it is to evaluate each response present during optimization, the more computationally expensive, and possible more complex, the design problem becomes.

For example, the minimum weight design of a wing, with fully coupled structural and aerodynamic models, is significantly more complex than considering the same problem with a static tip load. Similarly, analyzing non-linear post-buckling response of a structure is more complex than determining the linear bifurcation point. This means that an increased analysis complexity does not automatically result in a more complex optimization problem, however, a change in the nature of considered response may.

Model complexity is related to model fidelity and usually only effects the required computation time and the accuracy of the obtained response, the optimization problem remains essentially unchanged. For example, by generating a simplified model of the wing, the computational burden is reduced while the problem complexity remains the same. However, for variable stiffness laminates, if the design variables are associated with individual elements of finite element model, increasing model fidelity will result in a

more complex optimization problem due to an increased number of design variables.

Optimization complexity is influenced by the number of considered responses, number of design variables and their nature. Increasing the number of either the responses or the design variables inevitably increases design problem complexity and often affects the type of solution algorithms that can best be employed. The type of design variables and how they relate to the structural responses also greatly influences optimization problem complexity. Discrete design variables, such as the number of plies in a laminate, are notoriously difficult to handle using standard gradient based optimization techniques. Design variables which are interdependent also tend to render an optimization problem more complex. How response and design variables relate, in particular a linear versus non-linear relationship, also significantly influences the optimization problem complexity.

Several different optimization strategies are available and can roughly be classified into one of two categories: direct search methods and gradient based methods. Gradient-based methods make use of derivatives with respect to all design variables of the objective function and constraints to determine a descent direction. The complex nature of composite design often makes it difficult to evaluate meaningful gradient information. Direct search methods do not required derivative information and can therefore provide a useful outcome. Due to that, a Darwin Algorithm was chosen. An overview of the optimization tools that can be used for the design of variable stiffness composites laminates is provided in [37].

Here we will only attempt to highlight the basic concepts of the optimization tool that is used in the design process of this thesis.

3.2.1 Darwin Algorithm

ModelCenter has several algorithms available in the Optimization Tool. As said before; a Darwin algorithm was used for optimization.

Darwin is a genetic search algorithm developed specifically for solving engineering optimization problems. It is capable of handling discrete variables, continuous variables, and any number of constraints. Because Darwin does not require gradient information, it is able to effectively search non-linear and noisy design spaces. A penalty function is used to handle violated constraints. It uses elitist method to keep best designs from the previous generation.

To set up an optimization study using Darwin algorithm it is necessary to specify some control parameters, as shown in figure 3.4.

The first parameter is the **Population Size** which corresponds to the number of designs in each population. In general, the larger the population size, the longer the optimization process will run because of the increased number of component runs required. The population size should be initially set as small as possible and then slowly increased if it appears that the optimizer is not converging consistently to the best design.

The next parameter is the **Selection Scheme**. The genetic algorithm's selection scheme is the mechanism that determines which designs from the parent population and newly created child population will be chosen to make up the next generation of designs. The selection scheme ensures that the

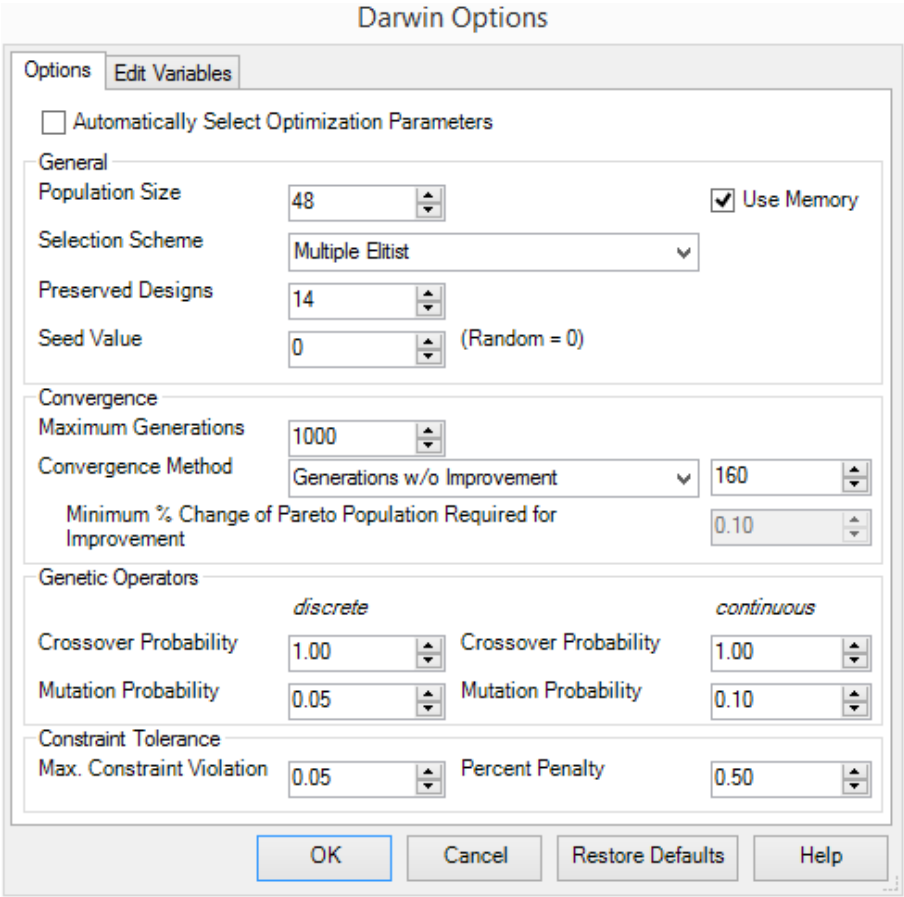

Figure 3.4: Darwin Options

optimization procedure continually progresses towards an optimal solution by allowing the best design(s) in each generation survive in the next generation.

Darwin utilizes two different types of selections schemes:**Elitist** and **Multiple Elitist** selection.

Elitist one takes the worst design from the child population and replaces it with the best design from the parent population. This method provides more of an explorative genetic search since each successive population is provided with a large number of new designs. Therefore, Elitist selection is generally effective for optimization problems with a single optimum point that is not surrounded by a large number of local optima. The potential problem with Elitist selection is that important genetic information that may exist in other desirable designs of the parent population is lost. Thus, it is probable that Elitist selection will be incapable of finding multiple global optimum points in the search space.

Multiple Elitist selection is more effective for problems where the search space has multiple global optimum points, or for problems where the global optimum is surrounded by many local optimum points. In Multiple Elitist selection, the parent and child populations are combined into one population and ranked. Members of the combined population are then arranged from best to worst according to their fitness values. The **Number of Preserved Designs,** N_p, specifies the number of best designs from the combined population that will be passed on to the next generation, and is used to control the selection pressure of the genetic algorithm.

N_p equal to the population size (maximum possible value of N_p) means that the next generation is

filled with the first half of the combined population and the procedure is complete.N_p less than population size means that the top Np designs from the combined population comprise the first part of the new generation. To fill the remainder of the new generation the ranked child population is searched, starting from the best design, for designs that have not already been passed on to the new generation. The first child found which is not located in the new generation is placed in first empty location in the new generation, and successive children fill out the rest of the new generation.

As the value of N_p increases, the number of new designs entering the population decreases,causing the genetic search to become more localized. Thus, using large values of N_p will prevent Darwin from exploring the design and may cause it to get trapped in a local optimum area of the search space. Therefore, the value of Np should be kept relatively small (less than 50%) compared to the population size so that a number of good designs can be tracked while maintaining a sufficient influx of new designs to continue searching other areas of the design space effectively.

The **Use Memory** parameter is a Darwin's memory feature used to help improve the overall efficiency of the design process. The memory feature works by storing each discrete design and its corresponding response information in a binary tree. This improves Darwin's efficiency by eliminating the need to re-analyze designs that are discovered more than once during the optimization process (research has shown that using a binary tree-based memory feature can improve overall efficiency of the GA procedure by 30% to 50% for designs with no continuous design variables). Selecting the Use Memory checkbox enables the memory feature. The one drawback of the memory feature is that it can use a significant amount of system memory when a large number of designs are stored in the binary tree.

The **Convergence** method also needs to be defined in the Darwin's Option.

There are two convergence methods that may be used to terminate the optimization process. The first method is to fix the number of generations that the optimizer will execute. This is done by selecting Fixed Generations from the convergence method drop down box. The number of generations that the optimizer will execute is then specified in the Maximum Generations field.

The second convergence method instructs the optimizer to continue until a user specified number of generations has been run without any improvement in the best design(s). This convergence method is specified by selecting Generations w/o Improvement from the convergence method drop down box and specifying the maximum number of generations without improvement in the field to the right of this drop down box.

For single-objective optimization, improvement is measured by the fitness of the best design. In this case, a counter is incremented by one if the top design in the current generations isn't better than the top design in the previous generation. If the counter reaches the value specified in the text field next to convergence method drop down box, the optimization procedure is terminated. The counter is reset to zero if the top design in the current generation is the best design found so far by Darwin.

When using the generations without improvement convergence criterion, the total number of generations that the optimizer will run is unknown, but will never exceed the number specified in the Maximum Generations text field.

Genetic Operators also need to be defined. The optimization algorithm implements each genetic

operator with its own specific probability, P. To determine whether or not a specific operator will be implemented, a uniformly distributed random number is created and compared against the operator's probability. If the random number is smaller than P, the operator is applied to the genetic string (s). The Crossover operator is typically applied with a high probability ($0.8 = P_c = 1.0$) because they are the genetic algorithm's primary means of traversing the search space. If crossover is not applied, then the parent strings are cloned into the child strings. Child strings are forced to be distinct from each other and from other designs in the parent population. If a distinct child cannot be found after a prescribed number of iterations, then one of the parents is cloned into the child population. The crossover process is repeated as many times as necessary to create a new population of designs.

Mutation performs the valuable task of preventing the premature loss of important genetic information by occasionally introducing random alterations in the genetic strings. Mutation is also needed because there is a low probability that the value at one or more locations in a design's genetic string will be identical to all other designs in the population as some point during an optimization run. Mutation is almost always applied with a low probability ($0.01 = P_m = 0.3$) and is implemented by changing, at random, a single value in the string to any other permissible value.

Finally, the Max Constrain Violation and the **Percent Penalty** need to be chosen.

In a genetic algorithm, designs are ranked (best to worst) according to their fitness. The fitness of a given design is generally expressed as:

$$fitness = objective + penalty \tag{3.3}$$

where objective is the value of the objective function, and a penalty is added to (or subtracted from) the objective function. If all of the design constraints are satisfied, the penalty term is zero. If one or more of the constraints is violated, the penalty is non-zero, and its magnitude is generally proportional to the magnitude of the constraint violation. It follows the basic function:

$$penalty = percent\_penalty \times (total\_constraint\_violation/max\_constraint\_violation)^{2.5} \tag{3.4}$$

Percent Penalty, specifies the percentage (e.g., $0.5 = 50\%$) by which the objective function will be penalized when the total constraint violation equals Maximum Constraint Violation. The penalty will be small for total constraint violations less than Maximum Constraint Violation, but will grow rapidly as the constraint violation exceeds Maximum Constraint Violation.

If the optimizer is rejecting designs that you think are acceptable, then Maximum Constraint Violation should be increased and/or Percent Penalty should be decreased. Likewise, if the optimizer is retaining designs that you think should be rejected, then Maximum Constraint Violation should be reduced and/or Percent Penalty should be increased.

All the control parameters here referred are in ModelCenter user's manual. For more details we refer the reader to the body of the manual [64].

Chapter 4

Optimum Blended Laminate Design Framework

As already said, this thesis aims to achieve a blended bi-stable laminate so that the performance of the structure can be maximized. To investigate that key parameters for laminate design need to be first defined.

1. Define the laminate geometry and its dimensions. Various geometries were tested: rectangular and trapezoidal laminates.

2. Define the boundary conditions of the structural problem. In this study, laminates arranged in a cantilever configuration are studied. To achieve this, a mixed lay-up showing symmetrical and unsymmetrical stacking sequences is used. The rectangular laminate is shown in figure 4.1.

3. Choose the laminate modeling philosophy that present the blending concept used to represent the fiber orientations of the continuous tow-paths.

4. Implement the tow-steering compatibility constraint. Here, the tow-steering compatibility constraint is introduced in the design methodology.

5. Define the design objective function that addresses the problem considered in this thesis by defining an appropriate objective function.

In this thesis, 4-ply thick laminates are considered within the top two plies having variable angle tow-steered configurations and the bottom two plies subjected to 0° fiber orientation over entire region. The non-bistable region, which represents the major structure near the perimeter of bi-stable section, has 0° fiber direction in each ply.

This chapter is divided in four sub-sections. Laminate Modeling Philosophy, Tow-steering Compatibility Constraint, Design Objective and Design Framework Implementation.

The description of the first two sub-sections will be based on the rectangular laminate considered in this thesis that is shown in detail in figure 4.1. However, it can be easily extended to the other geometry.

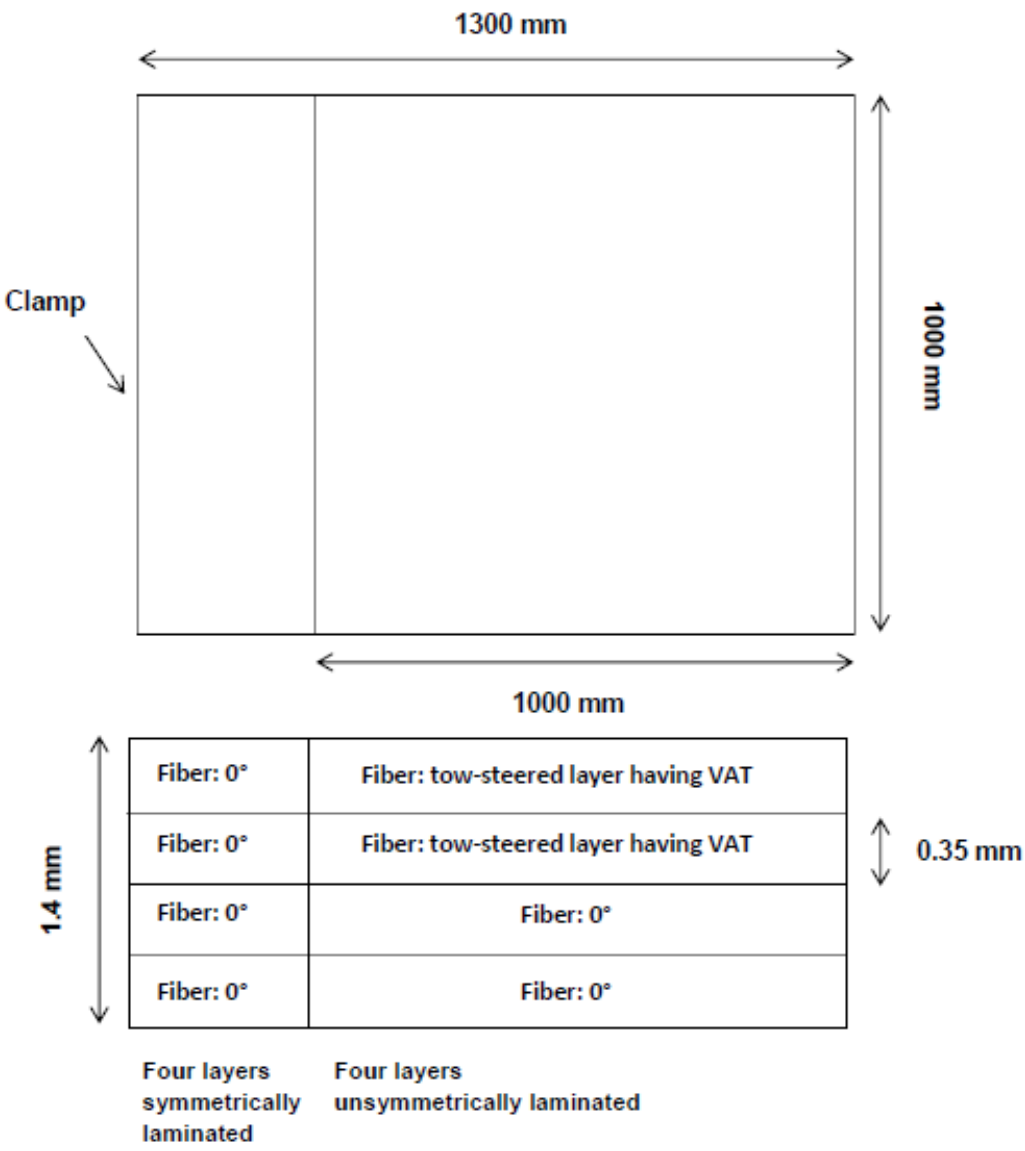

Figure 4.1: Planform ilustration of the rectengular bi-stable laminate

4.1 Laminate Modeling Philosophy

The focus of the modeling philosophy is to develop an efficient design for a variable stiffness bi-stable laminate, such that the advantages offered by the tow-steering techniques and composites materials are fully exploited.

The tow-steering technology uses equipment such as the Tajima TMLH-101 [65] to locally tailor fiber orientations across the planform of the laminate.

Tow-steered laminates with curved fiber paths can be designed to develop bistability in the structure along with ensuring fiber continuity within the wider structure, thereby structurally integrating the bi-stable section with the remaining structure.

However, allowing the use of variable stiffness laminates with arbitrary angles over the entire laminate significantly increase the design space due to the large number of associated design variables.

To make an effective use of the material properties of the laminate composite and in order to simplify the design space, it is useful to divide the structure into several segments. A rectangular panel can be used to demonstrate this concept, figure 4.2. Assume that p variables are needed to describe the material properties of the lay-up of one segment fully; hence there are at most p design variables if the panel were to be designed as using only a single segment. Dividing the part into q segments of a given dimension the design space is increased to pq design variables.

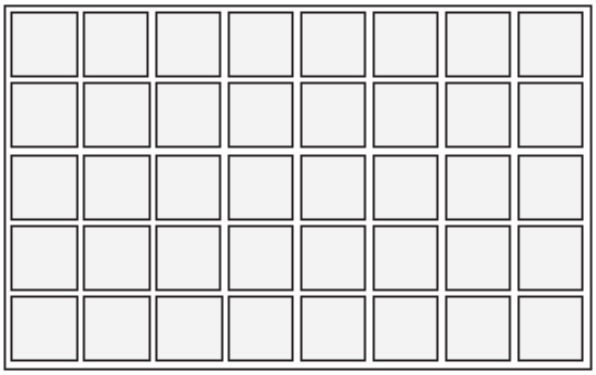

Figure 4.2: Rectangular panel divided in multiple segments

The segments of the structure can be progressively made smaller, to permit more design freedom, until they eventually converge towards the finite element representation.

A cellular based patch design approach was adopted. This consist in decompose the laminate into several patches/regions of straight-fibers to locally and discretely represent the fiber orientations of continuous tow paths generated by the tow-steering technique. The angle assigned to a region (cell) corresponds to the tow direction (averaged) within this region.

Figure 4.3 presents the blending concept, where the area enclosed by the edges BB', CC' are representative of the bistable region that will be optimized and the area enclosed by the edges AA', BB' represents the non-bistable region.

The bistable region has a cellular grid structure comprising 100 identical square cells (10(number of rows) x 10(number of columns)).

The cellular grid structure is decomposed into two sets of 5×10 sub-grids. The top grid is used for exploiting the possible combination of fiber angles while the bottom grid assumes anti-symmetric angles in the corresponding cells. In doing so, a nearly symmetric deformation can be achieved.

The fiber angles $\theta_{(R,C)}$ assigned to the cells in the top 5×10 grid are limited to possible values from the set $\{0^\circ$, 15° , 30° , 45° ,60° , 75° , $90^\circ\}$.

A general problem of designed tailored composite structures with multiple interconnected cells is that, the stacking sequence that results in the global optimum may lead to incompatibilities along adjacent cells. The resulting structure would suffer from stress concentrations at the boundaries between segments. For example, the forces in a ply with a discontinuity going from one cell to the other need to be transferred through the resin to adjacent plies which may induce failure of the matrix material. Enforcing stacking sequence continuity from one cell to another is generally referred to as blending.

In order to enforce compatibility of lamination sequences in adjacent cells and manufacturing limi-

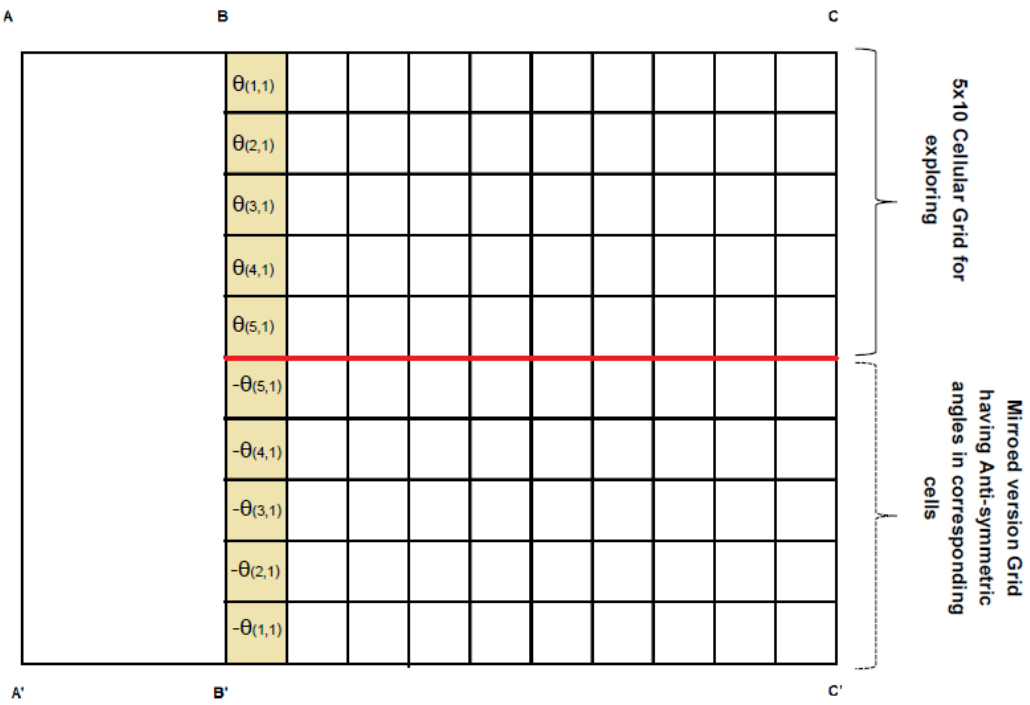

Figure 4.3: Laminate design philosophy

tations it is necessary to combine compatibility constrains with the cellular design approach. In doing so it is possible to obtain a closely-comparable tow-steered laminate with curvilinear fiber paths. The constraints inclusion will be exploited in the next section.

4.2 Tow-steering Compatibility Constraint

A tow-steering compatibility constraint was introduced in the design methodology to depict the continuous nature of the tow-steered construction in a cellular structure [36].

This constraint demands that each cell in the structure has fiber orientations not varying by an amount greater that $\theta adjoining$ from its adjoining cells.

This compatibility constrain can be expressed by the Inequality,

$$| \theta_{(R,C)} - \theta_{(U,V)} | \leq \theta adjoining \tag{4.1}$$

where $U = R-1, R, R+1; V = C-1, C, C+1;$ R and C are the number of the rows and columns, respectively.

Figure 4.4 schematically explain the meaning of inequality 4.1, the red cell is the one considered for constraint verification and the yellow cells are the adjoining cells for compatibility angle consideration.

The value of $\theta adjoining$ was selected as the double value of the angle increment between two consecutive values from the set of possible orientation angles referred in the previous sub-section. Saying that, $\theta adjoining = 30°$. This value of 30° is within the manufacturing capability of Tajima TMLH-101 for a cell dimension of $100mm \times 100mm$ [36].

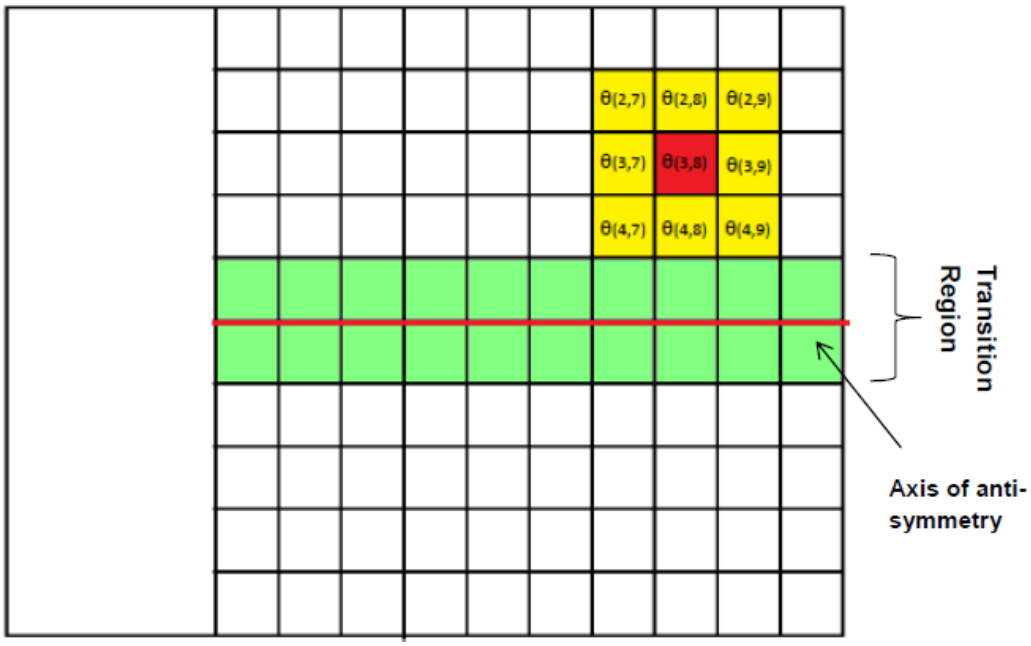

Figure 4.4: Tow-steering compatibility constraint and transition region

The introduction of this constrain means that the cells adjacent to the non-bistable region, $\theta_{(1to5,1)}$, are limited to possible values from the set $\{0^\circ$, 15° , $30^\circ\}$ since the non-bistable region has 0° fiber direction on each ply.

Moreover, the introduction of this constraint means that the higher value of fiber orientation angles in the cells adjacent to the axis of anti-symmetry, i.e,$\theta_{(5,1to10)}$ is 15° . This poses a limitation on the possibilities for laminate design and so a transition region was introduced.

In order to simplify the modelling of the transition region, the continuous arc representing the varying fiber directions was discretized in small cells. The equation 4.2 provides fiber angles corresponding to the average tangent direction of the circular arc inscribed in these discretized sub-regions (this expression was defined by Panesar et al. in [66]).

$$\theta_i = \theta_{bottom} + (\frac{\theta_{top} - \theta_{bottom}}{N+1}) \times i \tag{4.2}$$

where values of $i = 1, \ldots, N$ represent the fiber directions in the corresponding $20mm$ wide sub-regions, $i = 0$ represents the bottom most region,θ_{bottom}, and $i = N + 1$ represents the top most region, θ_{top}.

The orientation angles in that region are completely defined by the angle ,$\theta_{bottom} = -\theta_{top}$. The possible values of θ_{top} were chosen to be from the set $\{$ 0° , 15° , $30^\circ\}$ in the cell near the non-bistable region and from the set $\{$ 0° , 15° , 30° , 45° , $60^\circ\}$ in the remaining transition region.

For exemple, the computed θ_i values for the transition region with $\theta_{top} = 60^\circ$ and $\theta_{bottom} = -\theta_{top} = -60^\circ$ are $\{$-60° , -47° , -33° ,-20° , -7° ,7° , 20° , 33° ,47° , 60° $\}$ and are squematically represented in figure 4.5.

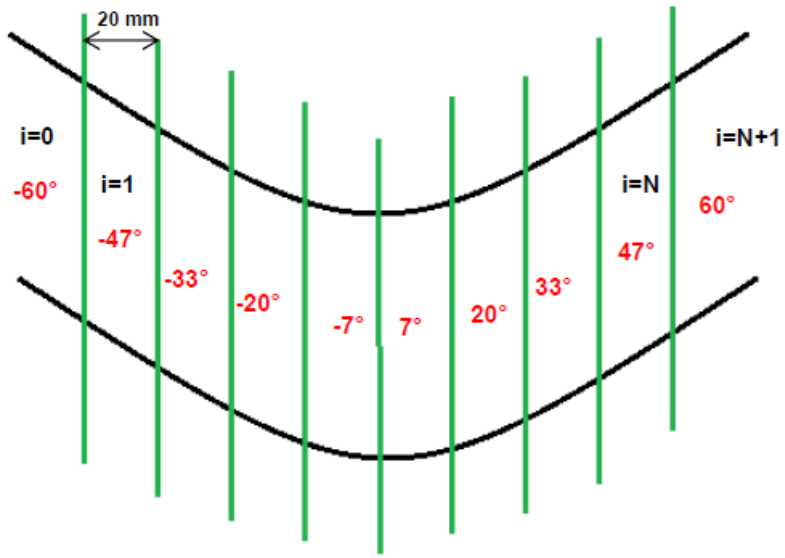

Figure 4.5: Transition region for case $\theta_{top} = 60°$

4.3 Design Objective

Clearly, with the ability to exploit the directional stiffness properties of composite materials, and tailoring of the structure shape, there is a scope for improving the bi-stable laminates for morphing and other applications.

The work presented in this thesis represents the effort to achieve the out-of-plane displacements suitable for a bi-stable laminate so that the performance of the structure can be maximized.

In order to meet the imposed requirements an appropriate design objective function must be chosen. The focus is to find the optimal fiber angles distribution that maximizes the relative deflections of the two stable states of a bi-stable composite.

The objective function may be explicitly defined in terms of out-of-plane displacements in stable state-1 (OPD1) and stable state-2 (OPD2), equation 4.3. The value used as the out-of-plane displacement value for a stable state is computed from the average value of the out-of-plane displacements of nodes C and mid-C, please refer to figure 4.3.

$$ObjectiveFuction = \begin{cases} \mid OPD1 \mid + \mid OPD2 \mid, & \text{if } OPD1 \leq 0 \, and \, OPD2 \geq 0 \\ 0, & \text{if } otherwise \end{cases} \tag{4.3}$$

4.4 Design Framework Implementation

In order to develop a design framework it is necessary to be able to: one, model the stiffness variation; two, analyze the structural response associated with the stiffness variation and three, optimize the design to meet the imposed requirements. It is suggested that the reader reviews one or more of the sections 2.4, 3.2 and 4.1, 4.2 and 4.3 if they require more information on a certain optimization option.

This sub-section describes the implementation of the design framework used for construct the opti-

mization problem and outlines the modeling tools used to execute each analysis.

This study considers the use of ModelCenter coupled with Abaqus FEA and Matlab to iteratively converge upon optimal designs in an automated fashion. The engineering design problem posed involves determining the out-of-plane displacements of a morphing bistable structure.

The design inputs are the fiber orientation angles and the objective is maximization of a function that quantifies the relative deflections of the two stable states of the structure.

Since the study involves changing the material properties of the above model, a fully parameterized Python script was written to automate the task in Abaqus. This script create the geometry, assembled the parts, applied the loads and boundary conditions, ran the analysis and exported relevant analysis information to a text file called Results.txt, all without any further user intervention.

The Python script was then wrapped using PHX ModelCenter's QuickWrap tool. Quickwrap automatically exposed the input variables in the Python script. It was also necessary to define the output variables and the file in which they are located, Results.txt. The command to run Abaqus then simply took the Python script as an argument and performed the steps in the script.

Then, it was needed to define constrain variables in order to enforce compatibility of lamination sequences in adjacent cells and manufacturing limitations, as described in the previous section 4.2. The inequality 4.1 is used to generate bounds for a given variable; such bounds are dynamic as they depend on the values of other design variables.

To achieve that a Matlab QuickWrap component that receive the design variables as input and generates constraint variables as out-put was created.

Considering the red cell of figure 4.4, 8 constraints need to be verified. However, this number can be reduced as the Darwin algorithm uses a penalty function to deal with the constraints. This means that the way of dealing with candidate solutions that violate constraints is to generate potential solutions without considering the constraints and then penalizing them by decreasing the "goodness" of the evaluation function. In other words, a constrained problem is transformed to an unconstrained problem by associating a penalty with all constraints violations and the penalties are included in the function evaluation.

That is, in pratical terms, it does not matter if only one or the eight constraints are not being verified since we are not interested in any of the solutions. Thus, instead of define 8 constraints is enough to define one.

The Matlab script begins by creating two variables called 'sub-constraints' given by equations 4.4a,b. Finally a global constraint is created. This constraint corresponds to the higher value of the two sub-constraints created earlier, equation 4.4c. Thus, each design variable must respect only one constraint (GlobalConstraint) in order to respect the inequality constraint expressed by equation 4.1.

$$\begin{aligned} SubConstraint_1 = \mid \theta_{(R,C)} - min(&\theta_{(R-1,C-1)}, \theta_{(R,C-1)}, \theta_{(R-1,C+1)}, \\ &\theta_{(R-1,C)}, \theta_{(R+1,C)}, \theta_{(R-1,C+1)}, \theta_{(R,C+1)}, \theta_{(R+1,C+1)}) \mid \end{aligned} \tag{4.4a}$$

$$SubConstraint_2 = \mid \theta_{(R,C)} - max(\theta_{(R-1,C-1)}, \theta_{(R,C-1)}, \theta_{(R-1,C+1)}, \theta_{(R-1,C)}, \theta_{(R+1,C)}, \theta_{(R-1,C+1)}, \theta_{(R,C+1)}, \theta_{(R+1,C+1)}) \mid \tag{4.4b}$$

$$GlobalConstraint = max(SubConstraint_1, SubConstraint_2) \tag{4.4c}$$

These two components define inputs and outputs that were used in the Optimization tool of ModelCenter. In ModelCenter the input variables are always treated as design variables, while output variables are treated either as constraints or as part of the objective.

To specify the variables it is just needed to drag the variables from the Component Tree and drop them into to Optimization Tool interface, as shown in figure 4.6. Each constraint has an upper bound that is equal to $\theta adjoining = 30°$.

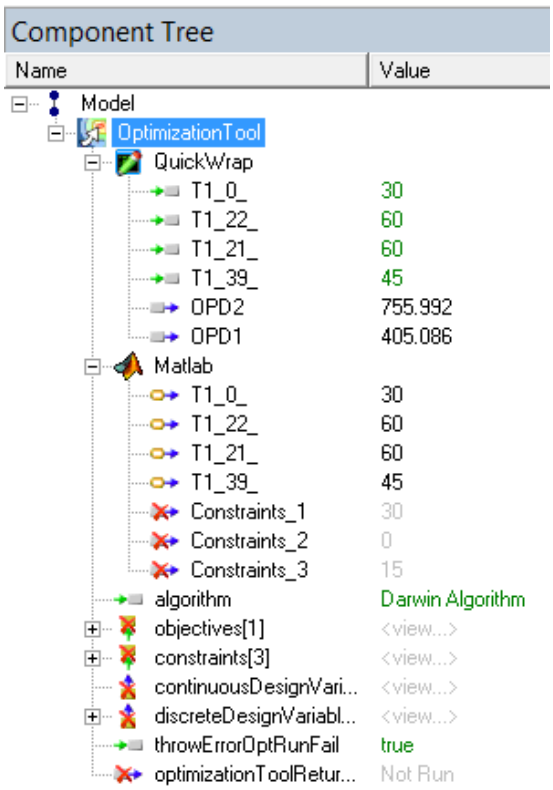

Figure 4.6: ModelCenter componente tree

The relationships between the three components of the model were established by linking them with the Link Editor. If variables have identical names links are automatically detected by ModelCenter.

The ModelCenter workflow setup is displayed in the following figure.

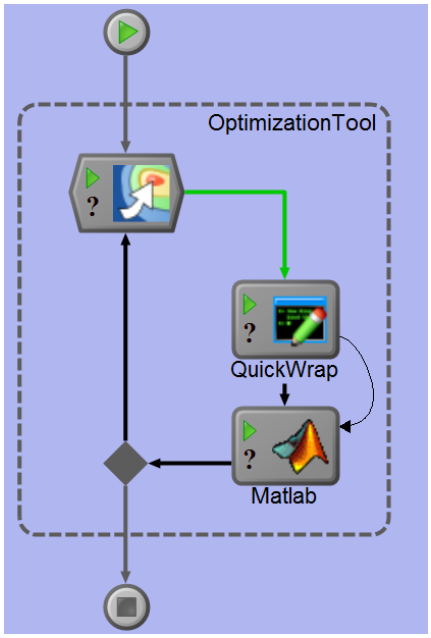

(a) The ModelCenter workflow

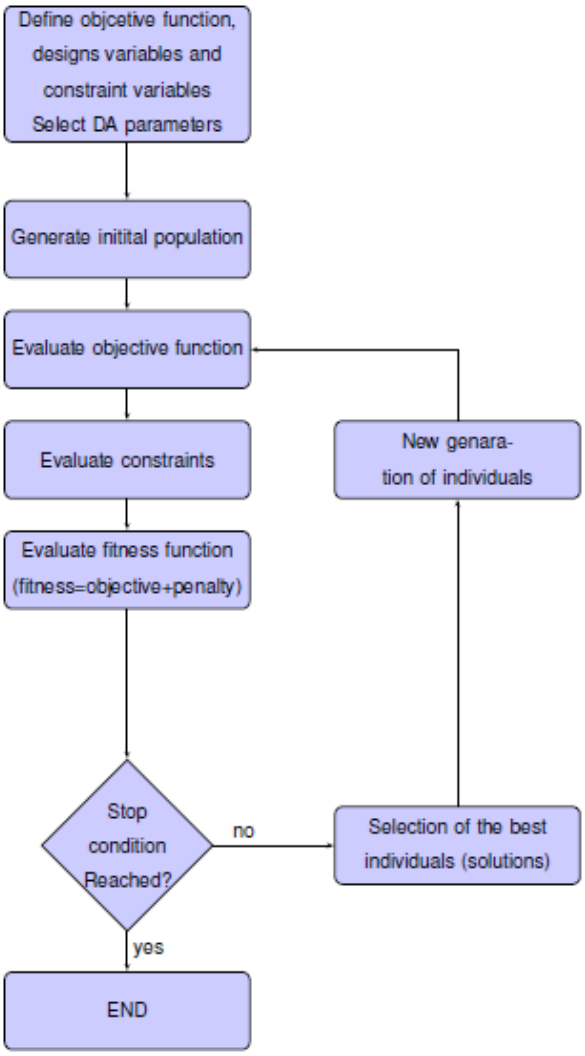

(b) Optimization scheme

Figure 4.7: Workflow and scheme

Chapter 5

Results Blended Laminate Design

This chapter presents a serie of numerical optimisation results using the problem formulation of Chapter 4. Two candidate designs are presented. These designs combine symmetric as well as unsymmetric layups. The first model is referred to as rectangular laminate and the second one as trapezoidal laminate.

The dimensions of different panel sections of the laminates designs are initial suggested values. Three different analyses were considered: one, a parametric study with only unidirectional fibers; two, a preliminary study that considers a less complex structure which could easily be tested within a short timespan; and three, a final study. The bistable equilibrium configurations developed and investigated in the present research could be used as an efficient structure for morphing wings.

All examples use T300/914 material properties, Table 5.1

Table 5.1: Material properties of carbon fiber laminates used throughout the analysis

Material	$E_{11}(GPa)$	$E_{22}(GPa)$	$G_{12}(GPa)$	υ	$\alpha_1(1/^\circ C)$	$\alpha_2(1/^\circ C)$	$t(mm)$
T300/914	130	10	4.4	0.3	-1.8e-8	30e-6	0.35

5.1 Rectangular Laminate

The steps used in the pseudo-dynamic FE analysis are described below and used a value of 5×10^-10 for the damping factor (unless stated otherwise):

1. In the first step residual stresses are introduced by cooling it to the room temperature. The cool-down is simulated by applying an initial temperature of 140° and a final temperature of 0° to all nodes of the model.$(c = 5 \times 10^-7)$

2. Actuation loads are applied on the corners C and C' to make the laminate deform in one of the stable shape of the laminate (see figure 4.2).

3. The loads are removed to acquire the first stable shape.

4. Actuation loads are now applied in the opposite direction to make the structure to snap-through and deform towards the possible second stable shape.

5. These loads are removed to observe a possible second stable shape.

Convergence study

Convergence studies were carried out to investigate the influence of both mesh density and the damping factor. Very fine meshes were computationally too demanding and extremely small damping factors resulted in models failing to converge.

The parameter considered for the convergence study is the out-of-plane displacement of the first stable state at room temperature. Different mesh sizes were used for the current study corresponding to total number of elements ranging from 216 to 11468. Meaning that each square segment of figure 5.5 were divided in 1x1, 2x2, 3x3, 4x4, 5x5, 6x6, 7x7, 8x8, 9x9 and 10x10 elements.

The convergence history plot for the out-of-plane displacement of the first stable is provided in figure 5.1.

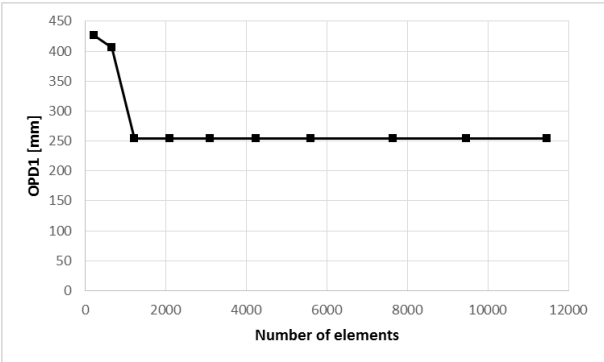

Figure 5.1: Convergence history in terms of out-of-plane displacement of the first stable state

A mesh of 1974 doubly-curved, 4 node shell elements, S4R, is used to perform the numerical analysis of the rectangular laminate in Abaqus. A good compromise between the model convergence and the computational effort was found for the reported values.

5.1.1 Unconstrained Parametric Study (Unidirectional Fibers)

The global optimum of the problem considered in this thesis is not intuitively obvious from the problem definition. Due to that, a first approach to the problem was done. This may allow us to understand how a variation on fiber orientation angles influences the objective function results.

A parametric study considering only unidirectional fibers was done. The study considers the set of fiber angles $\{15^\circ, 30^\circ, 45^\circ, 60^\circ, 75^\circ, 90^\circ\}$ for the top two plies of the bi-stable region, which is the one considered in the optimization process. The results of this analysis are reported in table 5.2.

It is important to note that this section presents the results for a design with no continuity constraints that intended to demonstrate the nature of the design space. This may allow us to make a measure

Table 5.2: Parametric study rectangular laminate

Fiber Orientation	15°	30°	45°	60°	75°	90°
Objective Function Results [mm]	910.1157	1017.516	**1084.861**	979.0173	966.9162	953.1396
OPD1 [mm]	387.4861	368.7811	**316.0459**	215.1117	220.8521	211.6232
OPD2 [mm]	522.6296	648.7351	**768.8154**	763.9056	746.0641	741.5164

of how the increased design freedom may lead to better results without taking in consideration the additional structural strength that results from using variable stiffness composites.

5.1.2 Preliminary Study

Problem description

In this section the optimization is performed to find the optimal distributions of fibers of a simplify model of the rectangular blended bi-stable laminate. This preliminary study has been conducted to test the developed design framework. This study also allows finding a possible initial fiber angle distribution to the final blended rectangular laminate.

In this preliminary study the bi-stable region is divided into 4 regions, as shown in figure 5.2. This results in a model with only four design variables.

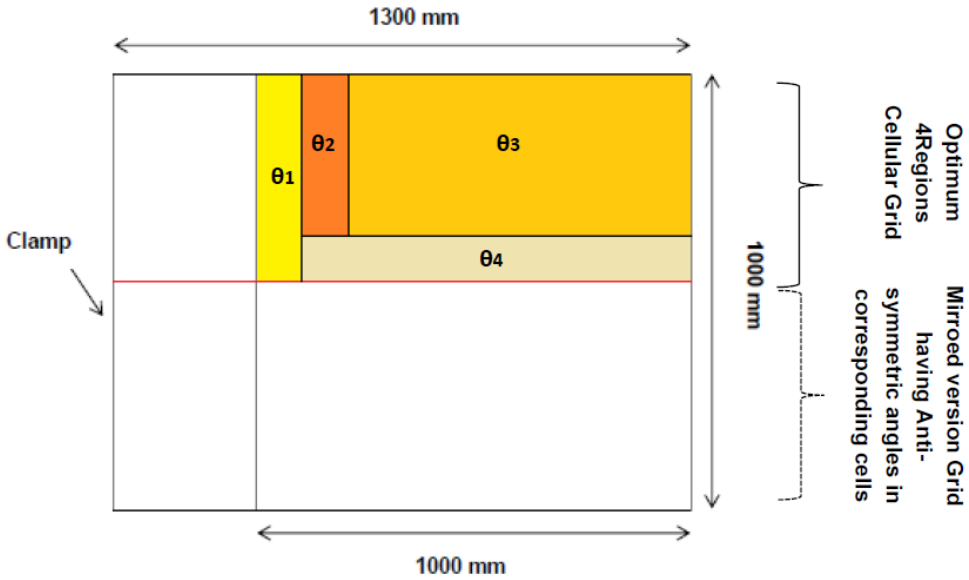

Figure 5.2: Preliminary model of the rectangular blended laminate

Region 1 is adjacent to the non-bistable section of the plate and can only have angles from the set $\{ 0°, 15°, 30° \}$. Region 2 is adjacent to region 1, thus the angle can take the values from the set $\{ 0°, 15°, 30°, 45°, 60° \}$. In region 3 the angles are limited from the set $\{ 0°, 15°, 30°, 45°, 60°, 75°, 90° \}$. Region 4 represents the transition region and the fibers angles are limited from the possible angles from the set $\{ 0°, 15°, 30°, 45°, 60° \}$.

The results of this preliminary study are reported in the following sub-section.

Generated Results

The Darwin algorithm was set to a population size of 21 with a multiple elitist selection scheme with a number of preserved designs $N_p = 6$. The Memory feature of the algorithm was used.

The algorithm was run until convergence, i.e. if the change in objective function value, equation 4.3 , isn't better than the top design in the previous generation for 20 consecutive iterations, or until a maximum number of iterations was reached. The number of maximum generations specified was 1000. A crossover probability of 1.00 and a mutation probability of 0.05 was used. The percentage penalty was set to 0.5.

Results were obtained using the out-of-plane displacements of the stable states of the plate according to equation 4.3, as a design objective.

The convergence study obtained for the maximum deflection between states is plotted in figure 5.3.

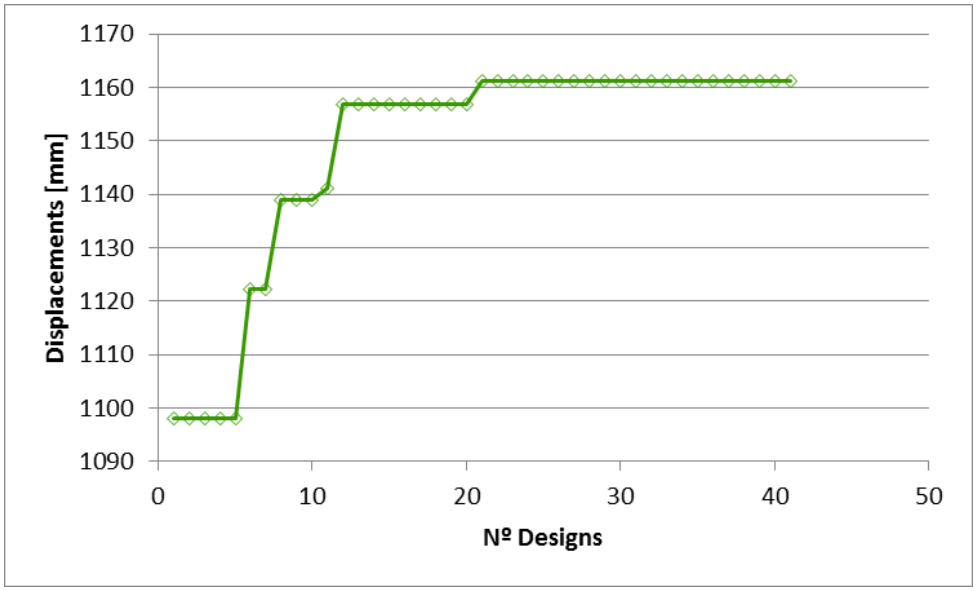

Figure 5.3: Design history of the preliminary study of the rectangular laminate

The best design was obtained for the fiber angles presented in figure 5.4. Note that the angles adjacent to the axis of anti-symmetry, i.e in the transition region are just the representative of the value of θ_{top}.

Table 5.3, reports the result OPD of each state as well as the result objective function,

Table 5.3: Results optimum preliminary design

	OPD1	OPD2
Displacements(mm)	405.086	755.992
Objective Funtion(mm)	1161.078	
No function calls	258	

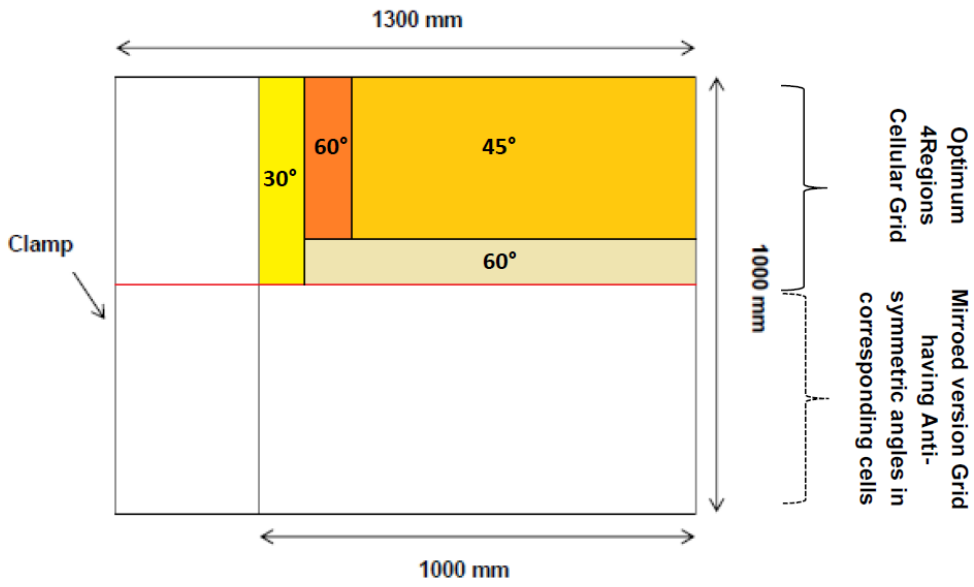

Figure 5.4: Optimum design of the preliminary study of the rectangular laminate

5.1.3 Final Blended Rectangular Laminate

Problem description

The rectangular laminates have the dimensions reported in figure 5.5. Each cell of the figure represents a fiber orientation angle, as explained in section 4.1.

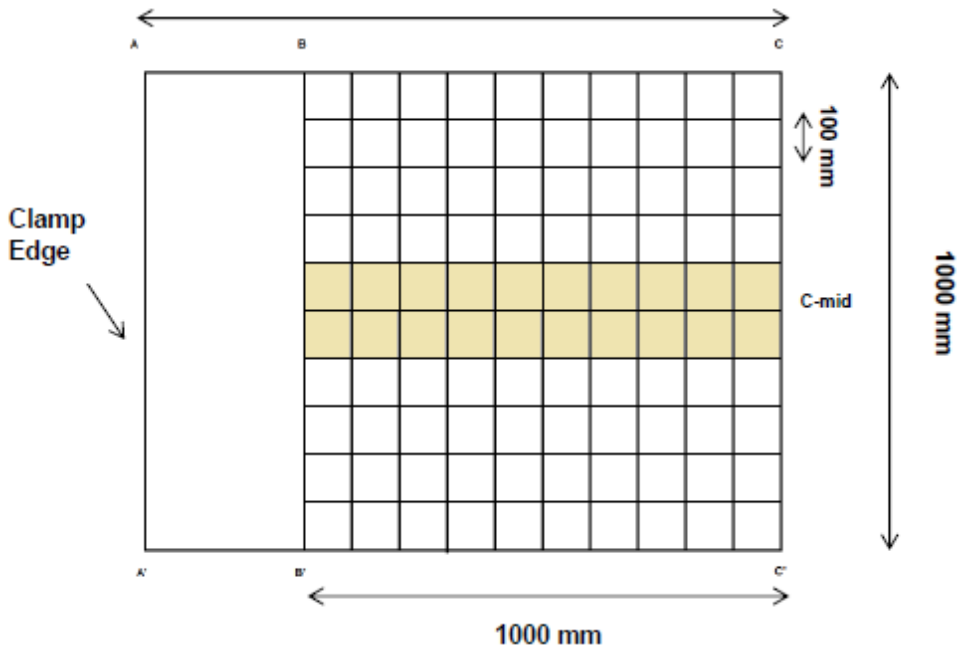

Figure 5.5: Rectangular laminate dimension and boundary conditions

The numerical predictions of the snap-through and snap-back are obtained by applying the boundary described in figure 5.5. A clamped boundary condition is imposed on the edge A-A'.

The generated optimum design obtained is reported in the following section. The numerical predic-

tion of snap-through and snap-back load is provided in section Numerical Results.

Generated results

The fiber angles $\theta_{(R,C)}$ assigned to the cells in the top 5×10 grid are limited to possible values from the set { 0° , 15° , 30° , 45° ,60° , 75° , 90° }. Note that the thickness of the laminate was kept constant.

The Darwin algorithm was set to a population size of 50 with a multiple elitist selection scheme with a number of preserved designs $N_p = 15$. The Memory feature of the algorithm was used.

The algorithm was run until convergence, i.e. if the change in objective function value, equation 4.3 , isn't better than the top design in the previous generation for 90 consecutive iterations, or until a maximum number of iterations was reached. The number of maximum generations specified was 1000. A crossover probability of 1.00 and a mutation probability of 0.10 was used. The percentage penalty was set to 0.5.

The initial fiber angle designs, or fiber angle seeds, used were the obtained in the previous preliminary study.

The convergence study obtained for the maximum deflection between states is plotted in figure 5.6.

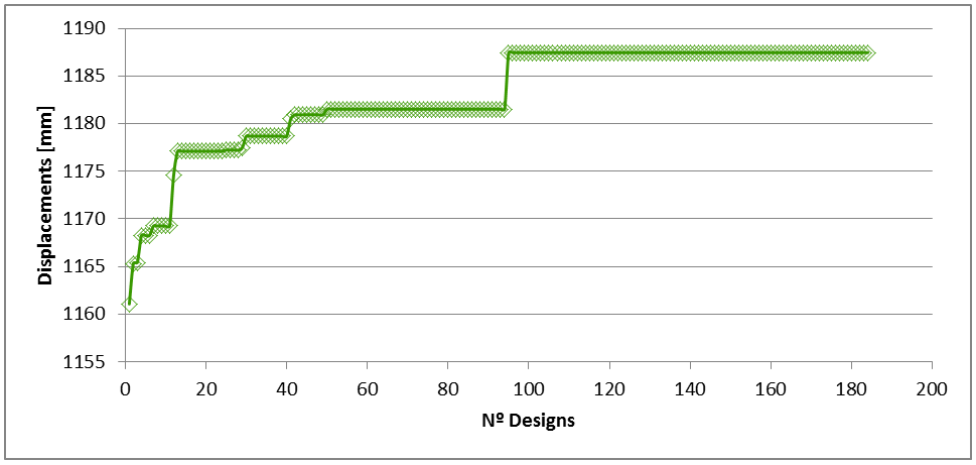

Figure 5.6: Design History Rectangular Laminate

The best design was obtained for the fiber angles presented in figure 5.7. Note that the angles adjacent to the axis of anti-symmetry, i.e in the transition region are just the representative of the value of θ_{top}. A discretized image of this transition region is provided in figure 5.8.

Finaly, a rough approximation of continuous curvilinear trajectories is provided in figure 5.9.

Numerical results

The numerical prediction of the optimum bi-stable laminate is provided in this section.

In figure5.10 it is possible to see the stable states of the obtained optimum design.

Table 5.4, reports the result OPD of each state as well as the result objective function,

The load-displacement plots allow us to compute the maximum out-of-plane load that the optimum laminates can withstand before changing configuration and are reported in figure 5.11. For convenience,

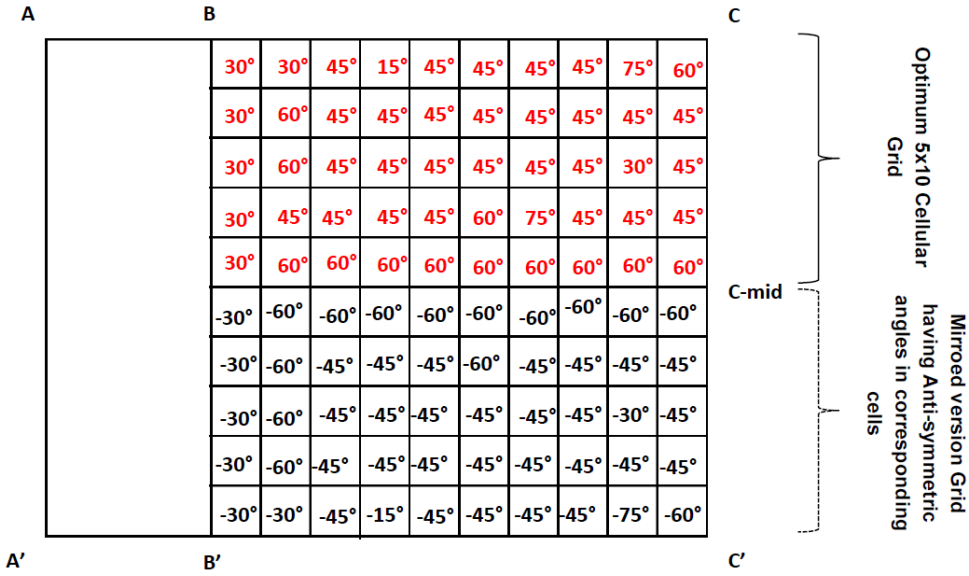

Figure 5.7: Optimum fiber angle distribution rectangular laminate

30°	60°	60°	60°	60°	60°	60°	60°	60°	60°
23°	47°	47°	47°	47°	47°	47°	47°	47°	47°
17°	33°	33°	33°	33°	33°	33°	33°	33°	33°
10°	20°	20°	20°	20°	20°	20°	20°	20°	20°
3°	7°	7°	7°	7°	7°	7°	7°	7°	7°
-3°	-7°	-7°	-7°	-7°	-7°	-7°	-7°	-7°	-7°
-10°	-20°	-20°	-20°	-20°	-20°	-20°	-20°	-20°	-20°
-17°	-33°	-33°	-33°	-33°	-33°	-33°	-33°	-33°	-33°
-23°	-47°	-47°	-47°	-47°	-47°	-47°	-47°	-47°	-47°
-30°	-60°	-60°	-60°	-60°	-60°	-60°	-60°	-60°	-60°

Figure 5.8: Transition region fiber angle distribution

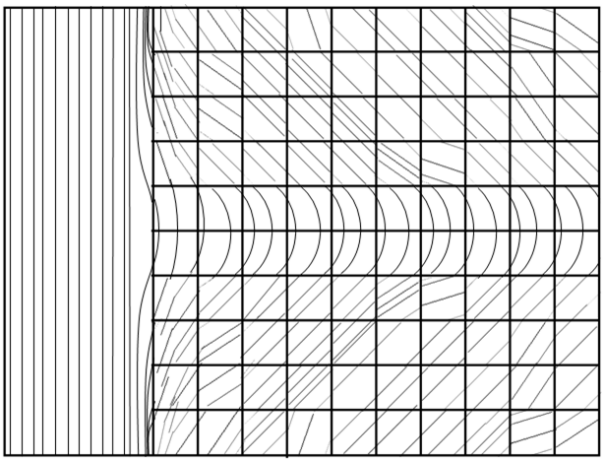

Figure 5.9: Approximation of continuous curvilinear trajectories rectangular laminate

Table 5.4: Results optimum design

	OPD1	OPD2
Displacements(mm)	438.941	748.525
Objective Funtion(mm)	1187.465	
No function calls	4532	

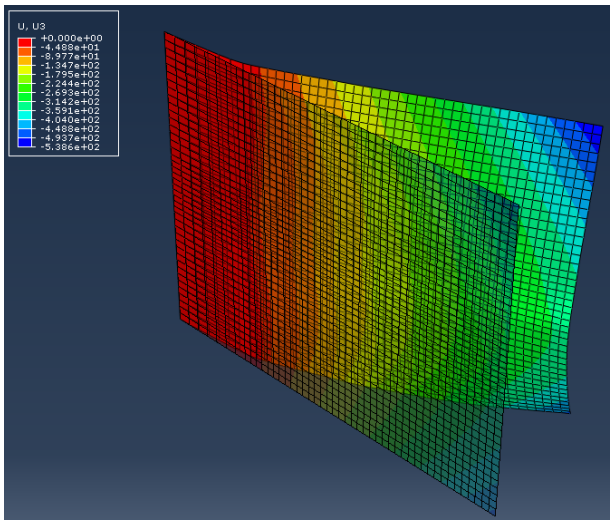

(a) Stable state 1

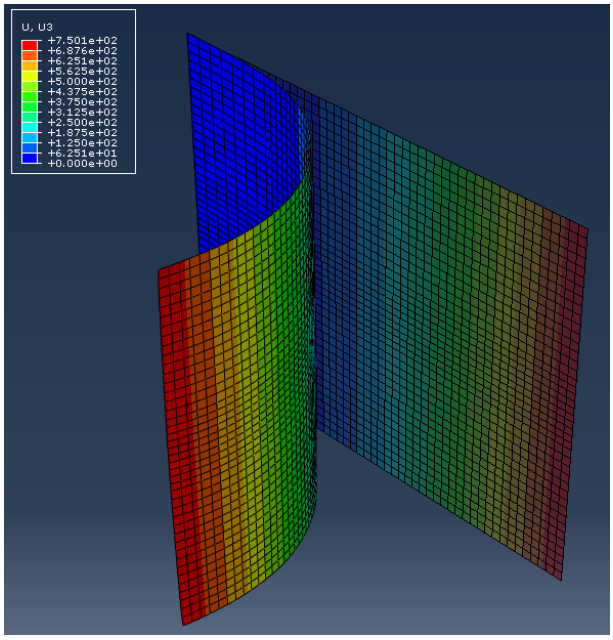

(b) Stable state 2

Figure 5.10: Stable states optimum rectangular laminate

it was defined that the first and second stable shapes as having negative and, respectively, positive values for the out-of-plane displacements. Thus, the actuation loads are acting in a positive direction to make the structure snap-through from the first to the second stable shape and in negative direction for opposite actuation.

5.2 Trapezoidal Laminate

The steps used in the pseudo-dynamic FE analysis are the same described in section 5.1.

Convergence study

As had been done with the rectangular laminate the parameter considered for the convergence study was the out-of-plane displacement of the first stable state at room temperature. Different mesh sizes

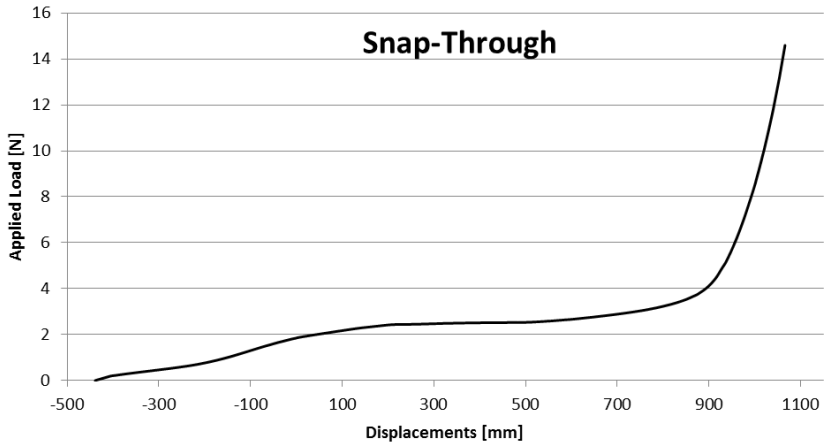

(a) Snap-Through

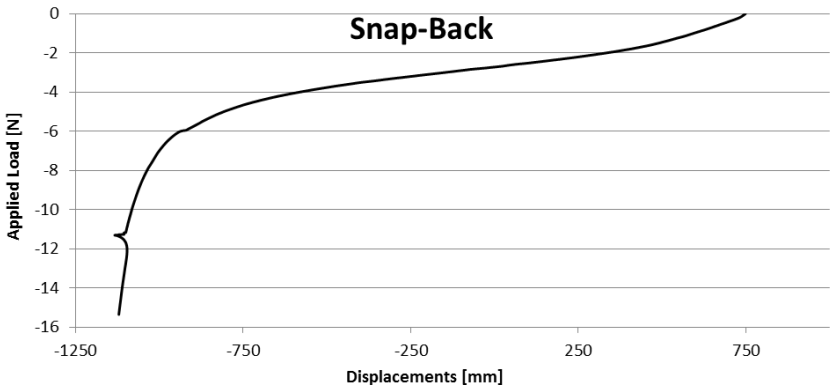

(b) Snap-Back

Figure 5.11: Load-displacement relationship

were used for the current study corresponding to total number of elements ranging from 582 to 10095. Meaning that each square segment of figure 5.16 were divided in 2x2, 3x3, 4x4, 5x5, 6x6, 7x7, 8x8, 9x9 and 10x10 elements.

The convergence history plot for the out-of-plane displacement of the first stable is provided in figure 5.12.

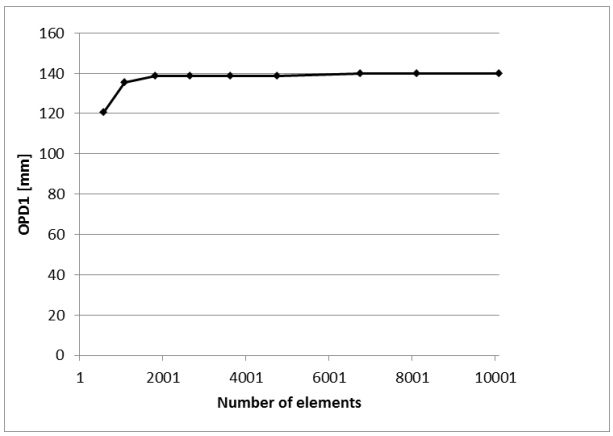

Figure 5.12: Convergence history in terms of out-of-plane displacement of the first stable state

A good compromise between the model convergence and the computational effort was found for a

mesh of 1698 doubly-curved, 4 node shell elements, S4R.

5.2.1 Unconstrained Parametric Study (Unidirectional Fibers)

As with the rectangular laminate a parametric study considering only unidirectional fibers was done. This study considers the set of fiber angles $\{15^\circ, 30^\circ, 45^\circ, 60^\circ, 75^\circ, 90^\circ\}$ for the top two plies of the bi-stable region, which is the set considered in the optimization process. The results of this analysis are reported in table 5.5.

Table 5.5: Parametric study trapezoidal laminate

Fiber Orientation	15°	30°	45°	60°	75°	90°
Objective Function Results [mm]	742.393	810.2612	886.0605	900.2391	**906.748**	0
OPD1 [mm]	283.4983	172.8987	134.7738	135.5509	**160.4721**	single state
OPD2 [mm]	458.8947	637.3625	751.2867	764.6882	**746.2759**	

It is important to note that this section presents the results for a design with no continuity constraints that intended to demonstrate the nature of the design space. This may allow us to make a measure of how the increased design freedom may lead to better results without taking in consideration the additional structural strength that results from using variable stiffness composites.

5.2.2 Preliminary Study

Problem description

As had been done with the rectangular geometry a preliminary analysis of a simple model of the bi-stable variable stiffness laminate was carried out.

The regions considered in this preliminary study are shown in figure 5.13 as well as the dimensions of the trapezoidal laminate regarded in this work.

Generated Results

The Darwin algorithm was set to a population size of 21 with a multiple elitist selection scheme with a number of preserved designs $N_p = 6$. The Memory feature of the algorithm was used.

The algorithm was run until convergence, i.e. if the change in objective function isn't better than the top design in the previous generation for 20 consecutive iterations, or until a maximum number of iterations was reached. The number of maximum generations specified was 1000. A crossover probability of 1.00 and a mutation probability of 0.05 was used. The percentage penalty was set to 0.5.

The convergence history obtained for the maximum deflection between states is plotted in figure 5.14.

The best design was obtained for the fiber angles presented in figure 5.15.

Table 5.6 , reports the result OPD of each state as well as the result objective function,

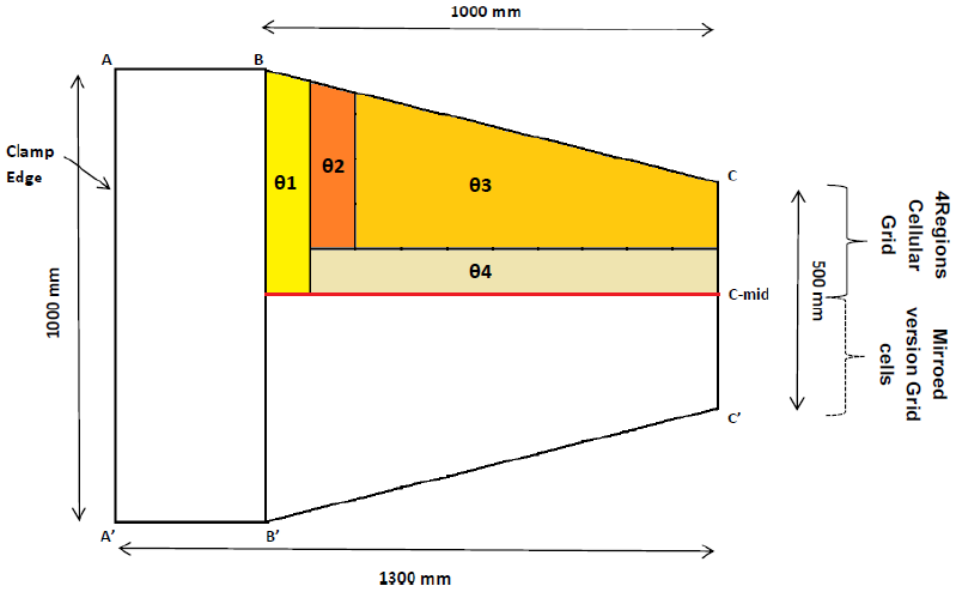

Figure 5.13: Preliminary model of the trapezoidal blended laminate

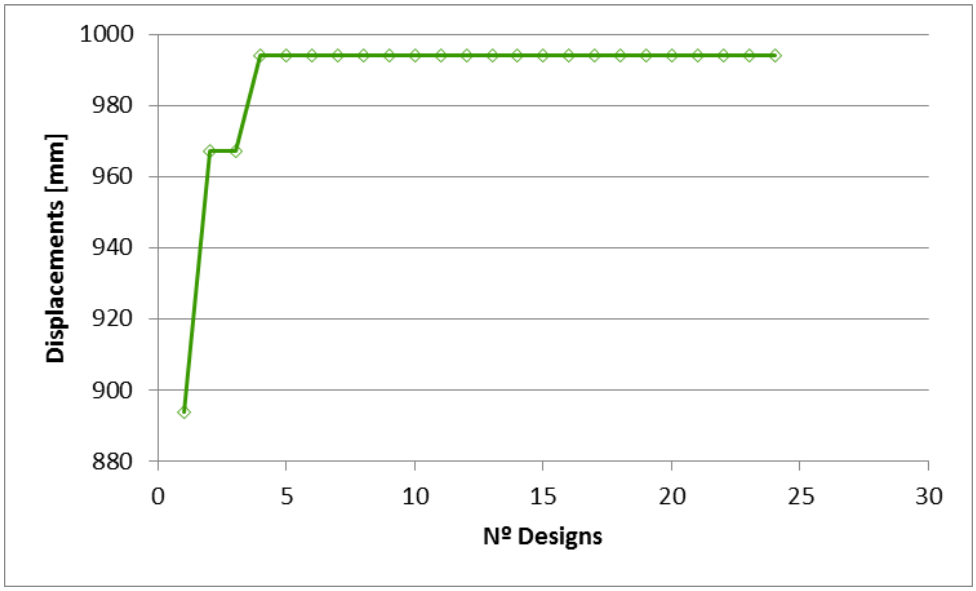

Figure 5.14: Design history of the preliminary study of the trapezoidal laminate

Table 5.6: Results optimum preliminary design

	OPD1	OPD2
Displacements(mm)	256.4093	737.7249
Objective Funtion(mm)	994.1342	
No function calls	170	

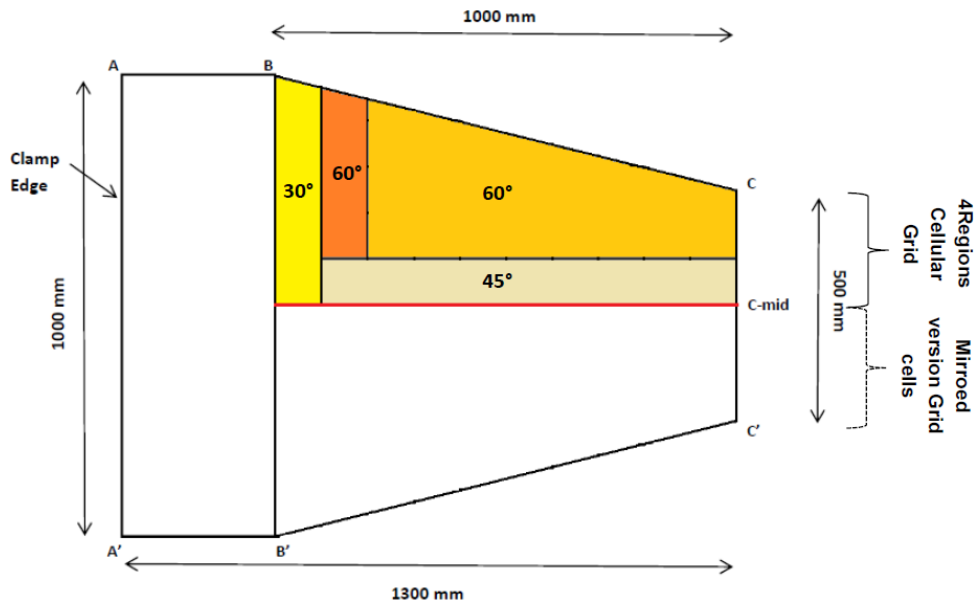

Figure 5.15: Optimum design of the preliminary study of the trapezoidal laminate

5.2.3 Final Blended Trapezoidal Laminate

Problem description

The regions considered in the final study of the trapezoidal laminate are reported in figure 5.16. The colored area represents the transition region.

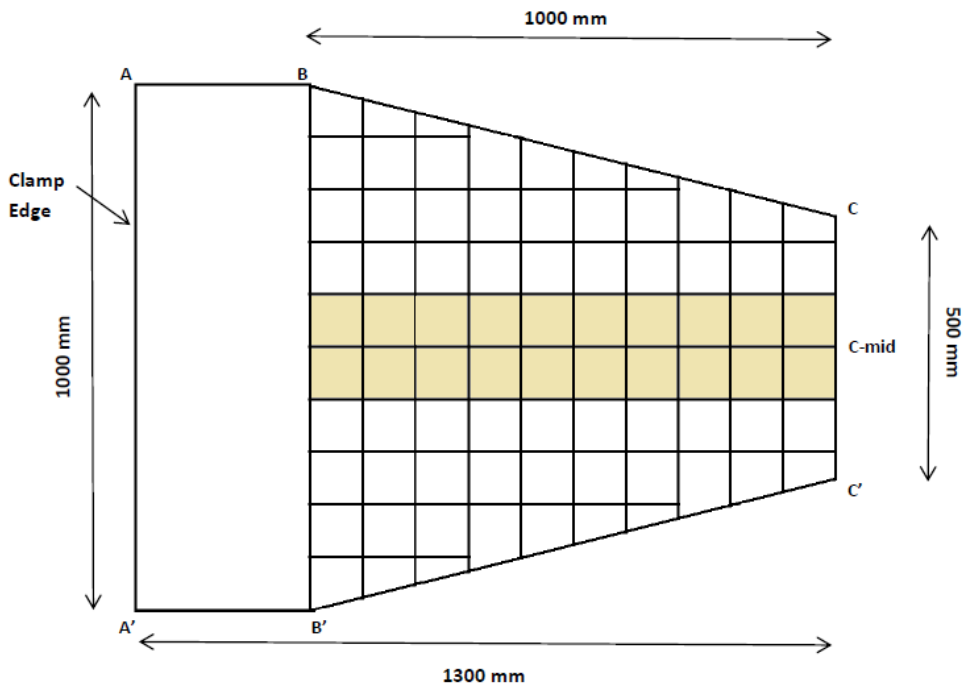

Figure 5.16: Trapezoidal laminate dimension and boundary conditions

The generated results are reported in the following section and the numerical predictions in the corresponding subsection.

Generated results

The fiber angles $\theta_{(R,C)}$ assigned to the cells in the top 5×10 grid are limited to possible values from the set { 0° , 15° , 30° , 45° ,60° , 75° , 90° }. Once again, the thickness of the laminate was kept constant.

The Darwin algorithm was set to a population size of 50 with a multiple elitist selection scheme with a number of preserved designs $N_p = 15$. The Memory feature of the algorithm was used.

The algorithm was run until convergence, i.e. if the change in objective function value, equation 4.3 , isn't better than the top design in the previous generation for 90 consecutive iterations, or until a maximum number of iterations was reached. The number of maximum generations specified was 1000. A crossover probability of 1.00 and a mutation probability of 0.10 was used. The percentage penalty was set to 0.5.

The initial fiber angle designs, or fiber angle seeds, used were the ones obtained in the preliminary study.

The convergence study obtained for the maximum deflection between states is plotted in figure 5.17.

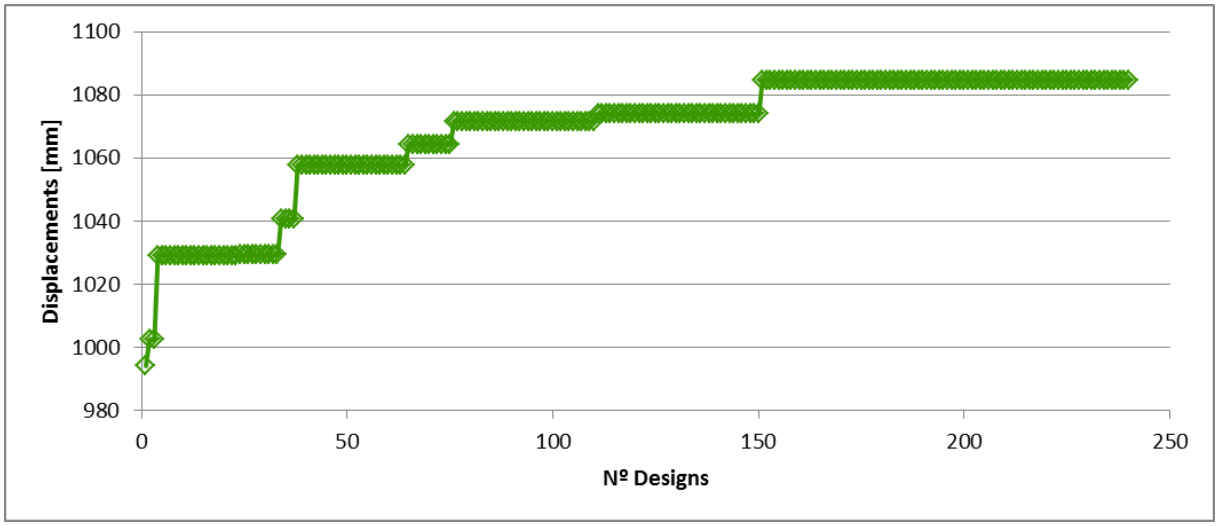

Figure 5.17: Design History Trapezoidal Laminate

The best design was obtained for the fiber angles presented in figure 5.18.

A discretized image of the transition region is provided in figure 5.19.

Finaly, a rough approximation of continuous curvilinear trajectories is provided in figure 5.20.

Numerical results

In figure 5.21 it is possible to see the stable states of the obtained optimum design.

Table 5.7, reports the result OPD of each state as well as the result objective function.

The load-displacement plots are reported in figure 5.22.

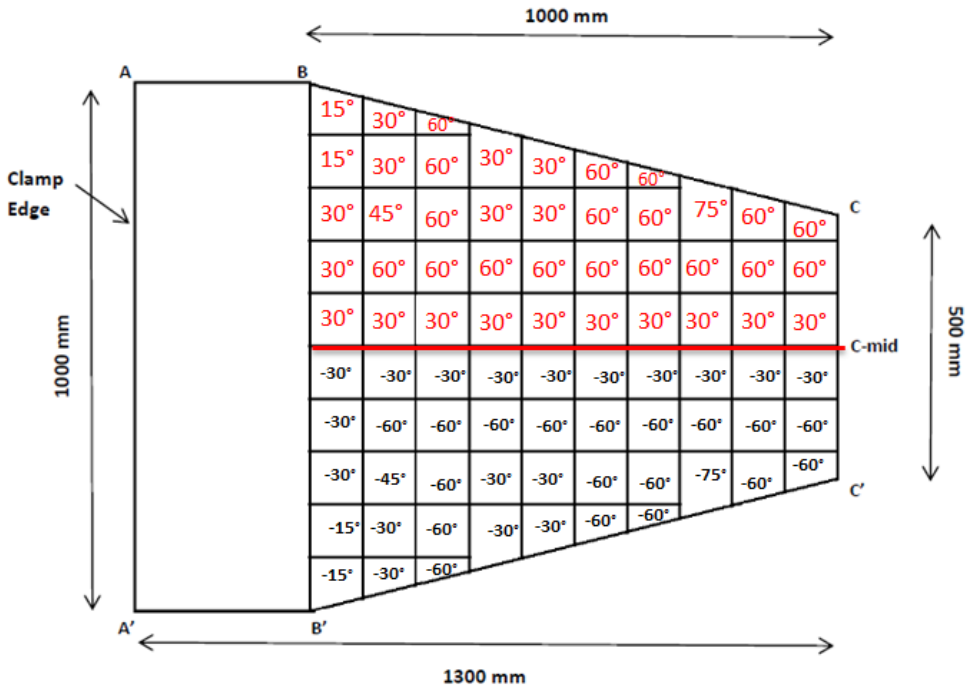

Figure 5.18: Optimum fiber angle distribution trapezoidal laminate

30°	30°	30°	30°	30°	30°	30°	30°	30°	30°
23°	23°	23°	23°	23°	23°	23°	23°	23°	23°
17°	17°	17°	17°	17°	17°	17°	17°	17°	17°
10°	10°	10°	10°	10°	10°	10°	10°	10°	10°
3°	3°	3°	3°	3°	3°	3°	3°	3°	3°
-3°	-3°	-3°	-3°	-3°	-3°	-3°	-3°	-3°	-3°
-10°	-10°	-10°	-10°	-10°	-10°	-10°	-10°	-10°	-10°
-17°	-17°	-17°	-17°	-17°	-17°	-17°	-17°	-17°	-17°
-23°	-23°	-23°	-23°	-23°	-23°	-23°	-23°	-23°	-23°
-30°	-30°	-30°	-30°	-30°	-30°	-30°	-30°	-30°	-30°

Figure 5.19: Transition region fiber angle distribution

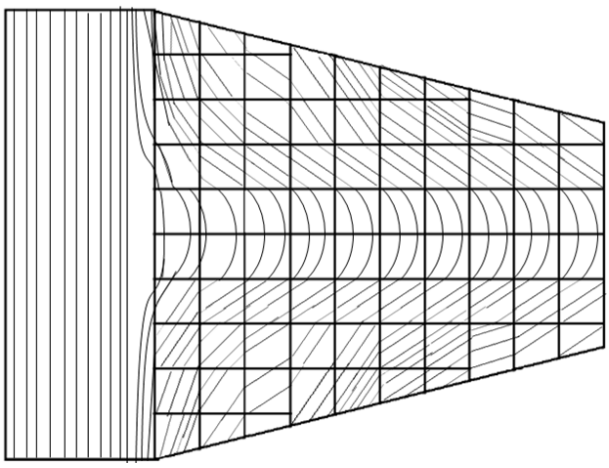

Figure 5.20: Approximation of continuous curvilinear trajectories trapezoidal laminate

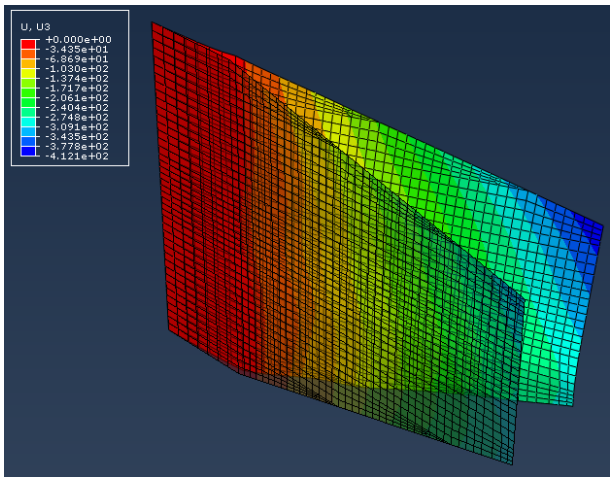

(a) Stable state 1

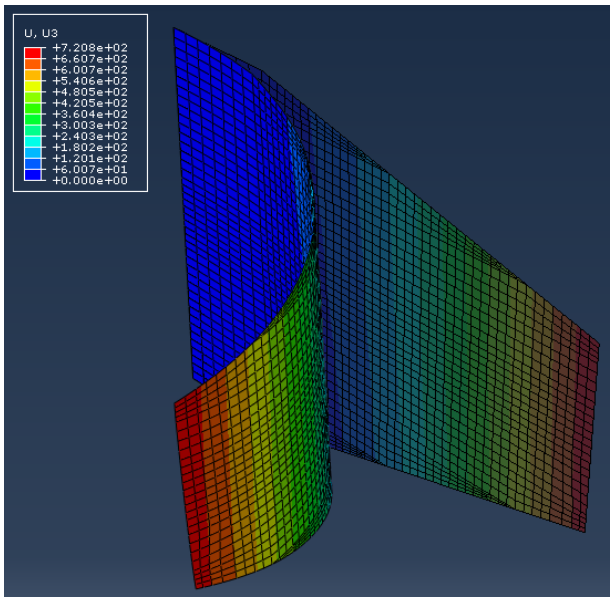

(b) Stable state 2

Figure 5.21: Stable states optimum trapezoidal laminate

Table 5.7: Results optimum design

	OPD1	OPD2
Displacements(mm)	367.7187	716.9683
Objective Funtion(mm)	1084.687	
No function calls	6020	

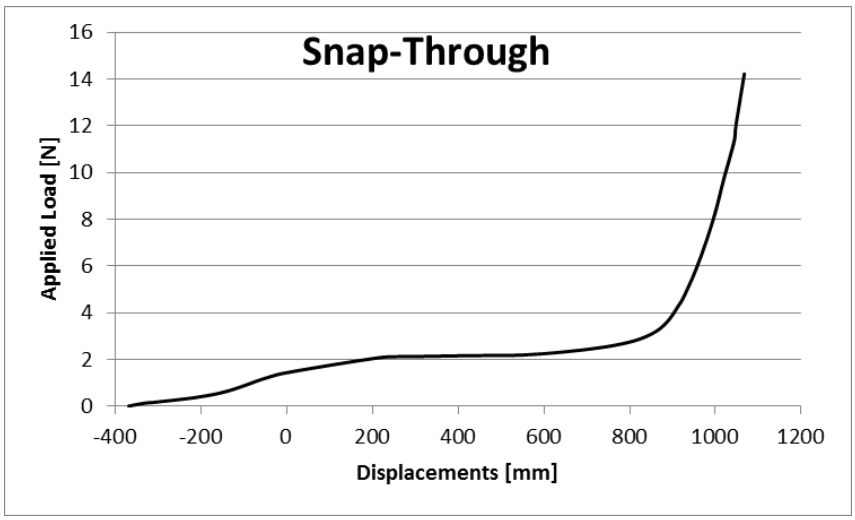

(a) Snap-Through

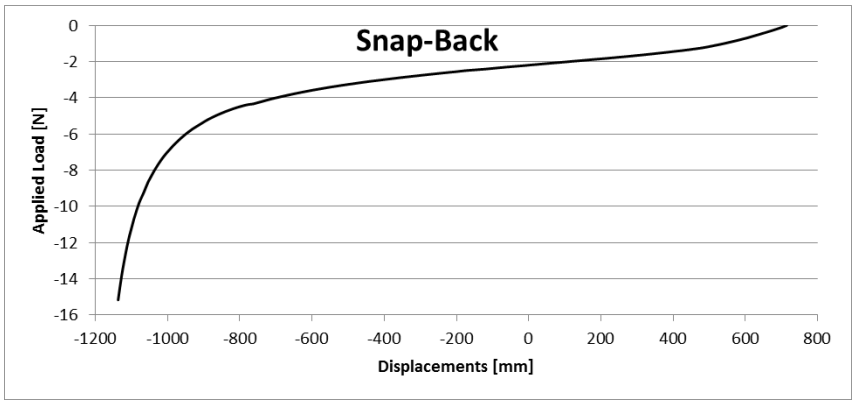

(b) Snap-Back

Figure 5.22: Load-displacement relationship

Chapter 6

Conclusions and Future Work

This chapter summarizes the main conclusions of this work and includes a discussion on a number of potential paths for future work.

6.1 Conclusions

The research performed in this thesis consisted in designing and realizing adaptive aircraft control structures by exploiting the directional stiffness properties of multistable composites. Multistable variable stiffness composites offer the potential to create structures that have the potential of being lighter and simpler than conventional control mechanisms as well as enabling geometric changes which would not traditionally be simple to achieve.

The document presents a design optimization framework used to devise morphing bi-stable laminates, where the laminates have been assumed to have variable stiffness. This framework take the advantages offered by-tow-steering techniques and composite materials while ensuring fiber continuity within the global structure. This was accomplished by using laminates with two regions with different stacking sequences. In doing so, it is possible to simulate the interaction between a moving component and a rigid structure that is applicable to morphing structures.

Two methods to design a variable stiffness laminate have been discussed in this thesis: a discrete patch design and a continuous design that use a curvilinear function to describe the fiber paths. An approach that combines these two techniques into a unified design approach was adopted given the designer more control over the steered variable stiffness composite layup.

The extended modelling was coupled to an optimization study where the objective function maximizes the performance of the bi-stable laminates considered. The design optimization framework consists of ModelCenter coupled with Abaqus FEA and Matlab to iteratively converge upon optimal designs in an automated fashion.

Different configurations of laminates geometries (rectangular and trapezoidal) and modeling approaches have been analyzed which include predicting their cured shapes and their stability characteristics due to a concentrate force leading to establishing the requirements to trigger snap-through

behaviour.

It is important to note that the simplified preliminary works of sections 5.1.2 and 5.2.2 provided a close approximation to the more complex cases. Quantitatively, i.e, in terms of the optimum solution's objective function value, the global study of figure 5.7 provided a 2% higher value than that of the preliminary solution of figure 5.4. The global solution of the trapezoidal laminate provided a 9% higher value than that of its preliminary study (figure 5.18 and 5.15, respectively).

For the parametric studies that were made using unidirectional fibers (sections 5.1.1 and 5.2.1) and again, taking into account the value of the objective function of each solution, improvement in the order of 10% were obtained in the case of the optimum rectangular laminate and 20% for the optimum trapezoidal laminate. This analysis allows us to quantify the increased design freedom that results from using a variable stiffness composites to improve the performance of the laminates considered. Moreover, the use of laminates with curved fibers mitigate the effect of stress concentrations that is expected to occur when straight fibers are used (due to the lay-up mismatch).

The Load-displacement graphics of the optimum rectangular and trapezoidal laminates were observed to compute the maximum out-of plane load that the laminates can withstand before changing configuration.

From the modelling viewpoint, and with optimization in mind, this mechanical force represents a simple mechanism which can be built on existing analysis. However the need for external mechanisms or additional support structures is not ideal and perhaps does not fit the ethos of morphing/smart structures. This mechanical actuation mechanism is present as a proof of concept, discussed as a first step towards understanding smart actuation.

Figures 5.11 and 5.22 show the relationship between the concentrated actuation loads applied to make the structure snap-through and the out-of-plane displacements. For convenience, it was defined that the first and second stable shapes as having negative and, respectively, positive values for the out-of-plane displacements. Thus, the actuation loads are acting in a positive direction to make the structure snap-through from the first to the second stable shape and in negative direction for opposite actuation. The snap-through loads can be defined as the loads for which large displacements occur. In the figures, these large displacements appear as the regions where the lines are horizontal.

The results reported here highlighting the effectiveness of the adopted optimization based methodology for studying sensitive yet non-convex optimisation problems.

Although the design framework proposed in this study is efficient in the maximization of the performance of bi-stable composites, it cannot be considered efficient in a computational point of view. In order to enable optimization studies for the design of bi-stable laminates the stable states need to be calculated at many design iterations. Fast and robust modelling techniques not currently exist for general bi-stable laminates.

Therefore, it can be concluded that the present work provides a valuable design tool based on the maximum relative deflections of a bi-stable composite for a wide range of morphing aircraft design applications such as winglets and wing camber. The learning outcome and the data obtained in this work are unavailable in the open literature, although there is considerable work done in the prediction of

post-cure shapes of unsymmetrical laminates.

The overall conclusion is that a versatile computational tool framework has been developed which can be used for the synthesis of optimal variable stiffness bi-stable composites based on optimal curvilinear finer paths and angles distribution.

6.2 Future Work

The developed optimization framework seems to be an efficient design tool for a preliminary investigation of optimum bi-stable composite structures. However, several challenges remain to be addressed.

Experimental studies

Future experimental studies to the designs conducted in this work should involve manufacture of the optimum designs for comparison. This experimental comparison would provide an evaluation and validation process for the design framework implemented.

Smart Actuation

If this structural deformation is to be realized in practical applications, some method of actuating the laminate must be included in the structure and accurately modelled. Many potential devices can be incorporated such as piezoelectric devices [51], shape memory alloys [50], and electrical drives [67].

Dynamic analysis

The work presented in this thesis has considered the behaviour of bi-stable laminates in static analysis only. This is ideal in as the focus has been on the overall deformation between two states, with no concern for the behaviour during actuation. In a study where the results are to be applied to a practical morphing application a dynamic understanding of the laminate behaviour is essential. For example, in aerospace applications the unstable transition between states could be a critical design consideration.

Optimization of bi-stable laminates

The computational issues associated with optimization of bi-stable composites present a challenge. The primary concern is the difficulty in obtaining a suitable initial guess, resulting in slow convergence to a solution or failure to capture the stable shapes. In order to progress with this research, there is a need to develop a more general approach to analyzing bi-stable laminate structures. This includes eliminating the need for a close estimate of the shapes to reliably capture the multiple solutions. Actually, while the numerical techniques are well suited to the analysis of a single laminate the problem is not well formed for optimisation where a fast and robust method is required for the calculation of bi-stable laminate characteristics at every design iteration. In an optimization routine where the design is constantly being updated, obtaining a close approximation of the shape is more difficult.

Bibliography

[1] Roeseler W Batzer R Baron W Velicki A. Renton WJ, Olcott D. Future of flight vehicle structures (2000–2023). *J Aircraft 41(5):986–97*, 2004.

[2] Schultz MR Hyer MW. A morphing concept based on unsymmetric composite laminates and piezoceramic mfc actuators. *45th AIAA/ASME/ASCE/AHS/ASC structures, structural dynamics and materials conference. AIAA paper no. 2004-1806*, April 2004.

[3] Pellegrino S. Kebadze E Guest SD. Bi-stable prestressed shell structures. *Int J Solids Struct*, 2004.

[4] Hyer MW. The room-temperature shapes of four layer unsymmetric cross-ply laminates. *Journal of Composite Materials 16*, 1982.

[5] A. E. Bergamini A. F. Arrieta, T. Delpero and P. Ermanni. Broadband vibration energy harvesting based on cantilevered piezoelectric bi-stable composites. *J. Applied Physics Letters 102, 173904 (2013); doi: 10.1063/1.4803918*, 2013.

[6] Hyer MW. Some observations on the cured shape of thin unsymmetric laminates. 1981.

[7] Hyer MW. Calculations of the room-temperature shapes of unsymmetric laminates. 1981.

[8] Hamamoto A. Hyer MW. Nonlinear temperature curvature relationships for unsymmetric graphite epoxy laminates. *Int J Solids Struct*, 1987.

[9] Dano ML Hyer MW. Thermally-induced deformation behavior of unsymmetric laminates. *Int J Solids Struct*, 1998.

[10] Wijskamp S. Akkerman R. Lamers EAD. Residual stresses in non-symmetrical carbon/epoxy laminates. *ICCM 14, International conference on composites: bridging the gap between academia and industry*, 2003.

[11] Cerami M. Weaver PM. Characterization of unsymmetric cross-ply laminate deflections using orthogonal polynomials. *49th AIAA/ASME/ASCE/AHS/ASC structures, structural dynamics, and materials conference*, 2008.

[12] Campanile LF. Smart shape control: using compliant and active materials to adapt structural geometry. challenges and good reasons. *14th international conference on adaptive structures and technologies(ICAST)*.

[13] Campanile LF. Light weight shape - adaptable airfoils: a new challenge for an old dream. adaptive structures: engineering applications. *John Wiley & Sons, Ltd.*, 2007.

[14] Leissa AW Martin AF. Vibration and buckling of rectangular composite plates with variable fiber spacing. *Compos Struct*, 1990.

[15] Curry JM Johnson ER Starnes JH. Effect of dropped plies on the strength of graphite–epoxy laminates. *Compos Struct*, 1992.

[16] Mattioni F. Diaconu CG, Weaver PM. Concepts for morphing airfoil sections using bi-stable laminated composite structures. *Thin-Walled Struct 46(6)*, 2008.

[17] Weaver PM Mattioni F. The application of residual stress tailoring of snapthrough composites for variable sweep wings. *47th AIAA/ASME/ASCE/AHS/ASC structures, structural dynamics, and materials conference, Newport,Rhode Island*, 2006.

[18] C.S. Sousa P.P. Camanho A. Suleman. Analysis of multistable variable stiffness composite plates. *Composite Structures 98*, 2013.

[19] Z. Gürdal R. Olmedo. In-plane response of laminates with spatially varying fibre orientations: Variable stiffness concept. *AIAA J., 31(4)*, 1993.

[20] Gürdal Z. Waldhart, C. and C. Ribbens. Analysis of tow placed, parallel fiber, variable stiffness laminates. *37th AIAA/ASME/ASCE/AHS/ASC Structures, Structural Dynamics, and Materials Conference*, 1996.

[21] Kelly D. Li, R. and A. Crosky. Strength improvement by fibre steering around a pin loaded hole. *Compos. Struct.*, 2013.

[22] Huang J Haftka RT. Optimization of fiber orientations near a hole for increased load-carrying capacity of composite laminates. *Struct Multidiscip Optim*, 2005.

[23] Tatting B. Gürdal, Z. and C. Wu. Variable stiffness composite panels: Effects of stiffness variation on the in-plane and buckling response. *Composites Part A 39*, 2008.

[24] Ijsselmuiden ST Gürdal Z. Setoodeh S, Abdalla MM. Design of variablestiffness composite panels for maximum buckling load. *Compos Struct 87*, 2008.

[25] Camanho PP. Lopes CS, Gürdal Z. Variable-stiffness composite panels: buckling and first-ply failure improvements over straight-fibre laminates. *Comput Struct*, 2008.

[26] Moura MFSF Akhavan H, Ribeiro P. Large deflection and stresses in variable stiffness composite laminates with curvilinear fibres. *Int J Mech Sci*, 2013.

[27] Stickler P. Blom, A. and Z. Gürdal. Optimization of a composite cylinder under bending by tailoring stiffness properties in circumferential direction. *Composites Part B 41*, 2010.

[28] De Breuker R. Abdalla, M. and Z. Gürdal. Aeroelastic tailoring of variablestiffness slender wings for minimum compliance. *nternational Forum on Aeroelasticity and Structural Dynamics (IFASD)*, 2007.

[29] Hol JMAM Blom AW, Setoodeh S. Design of variable-stiffness conical shells for maximum fundamental eigenfrequency. *Comput Struct*, 2008.

[30] SEDAT GÜLDÜ. Analysis and optimization of cylindrical structures manufactured by automated fiber placement technique. Master's thesis, SCHOOL OF NATURAL AND APPLIED SCIENCES OF MIDDLE EAST TECHNICAL UNIVERSITY, 2014.

[31] Vaniglia M. M. Evans, D. O. and P. C. Hopkins. Fiber placement process study. *34th International SAMPE Symposium*, May 1989.

[32] Alexander R. A. Buchanan, D. L. and J. A. Thomas. Structural design of a fiber placed inlet duct. *40th AIAA/ASME/ASCE/AHS/ASC Structures, Structural Dynamics and Materials Conference*, 1999.

[33] Wu KC. Thermal and structural performance of tow-placed, variable stiffness panels. *IOS Press*, 2006.

[34] W Hufenbach M Gude L Kroll A Sokolowski and B Werdermann. Adjustment of residual stresses in unsymmetric fiber reinforced composites using genetic algorithms. *Mechanics of Composite Materials,37*, 2001.

[35] W Hufenbach and M Gude. Analysis and optimisation of multistable composites under residual stresses. *Composite Structures , 55*, 2002.

[36] Weaver PM. Panesar AS. Optimization of blended bistable laminate for morphing flap. *51st AIAA/ASME/ASCE/AHS/ASC structures, structural dynamics, and materials conference*, 2010.

[37] Damiano Pasini Larry Lessard Hossein Ghiasi, Kazem Fayazbakhsh. Optimum stacking sequence design of composite materials part ii: Variable stiffness design. *Composite Structures, Volume 93, Issue 1*, 2010.

[38] Tsai S. and Hahn H. *Introduction to composite materials*. 1980.

[39] Kassapoglou C. *Design and Analysis of Composite Structures: With Applications to Aerospace Structures*. 2010.

[40] Weaver P.M. Potter K.D. Friswell M.I. Mattioni, F. Multi-stable composites application concept for morphing aircraft. *ICAST Conference, Paris,*, October, 2005.

[41] Gatto A. Weaver P. Friswell M. Potter K. Mattioni, F. The application of residual stress tailoring of snap- through composites for variable sweep wings. *14th AIAA/ASME/AHS Adaptive Structures Conference*, May 2006.

[42] J. N. Reddy. *Mechanics of Laminated Composite Plates*. 1997.

[43] BD Agarwal and LJ Broutman. *Analysis and Performance of Fiber Composites*. New York, USA, 1980.

[44] J. Dang and Y. Tang. Calculation of the room-temperature shapes of unsymmetric laminates. *International Symposium on Composite Materials and Structures, People's Republic of China*, 1986.

[45] W.J. Jun and C.S. Hong. Effect of residual shear strain on the cured shape of unsymmetric cross-ply thin laminates. *Journal of Composite Science and Technology*, 1990.

[46] W.J. Jun and C.S. Hong. Cured shapes of unsymmetric laminates with arbitrary lay-up angles. *Journal of Reinforced Plastics Composites*, 1992.

[47] Dassault Systemes Simulia Corp., Providence, RI, USA. *Abaqus/CAE User's Manual*, 2010.

[48] Potter KD Friswell MI. Mattioni F, Weaver PM. Analysis of thermally induced multistable composites. *Int J Solids Struct 45(2)*, 2008.

[49] M.W.Hyer M.L.Dano. Snap-through of unsymmetric fiber reinforced composite laminates. *International Journal of Solids and Structures 39*, 2002.

[50] M.W.Hyer M.L.Dano. Sma-induced snap-through of unsymmetric fiber-reinforced composite laminates. *International Journal of Solids and Structures 40*, 2003.

[51] P. M. Weaver I. P. Bond P. M. Portela, P. P. Camanho. Analysis of morphing multi-stable structures actuated by piezoelectric patches. *.A. Mota Soares, et al.(Eds.), Proceedings of the Second ECCOMAS Thematic Conference on Smart Structures and Materials*, July2005.

[52] Tan X. Ozbay S. Armanios E. Tawfik, S. Anticlastic stability modeling for cross-ply composites. *Journal of Composite Materials 41*, 2007.

[53] Charette R Hyer MW. The use of curvilinear fiber format in composite structure design. *AIAA 29:1011–5*, 1991.

[54] Abdelal GF. Abdalla MM, Gürdal Z. Thermomechanical response of variable stiffness composite panels. *Therm Stresses*, 2009.

[55] M.M. Abdalla Setoodeh and Z.Gürdal. Design of variable stiffness laminates using lamination parameters. *Composites, Part B: Engineering, 37*, 2006.

[56] Lopes CS Camanho PP Gürdal Z Tatting BF. Progressive failure analysis of tow-placed variable-stiffness composite panels. *Int J Solids Struct*, 2007.

[57] Tatting B Gürdal Z. Analysis and design of tow-steered variable stiffness composite laminates. *American helicopter society hampton roads chapter, structure specialists' meeting*, 2001.

[58] R. Olmedo and Z. Gürdal. Buckling response of laminates with spatially varying fiber orientations. *34th AIAA/ASME/ASCE/AHS/ASC Structures, Structural Dynamics and Materials Conference*, 1993.

[59] Setoodeh S. Hol J. Blom, A. and Z. Gürdal. Design of variable-stiffness conical shells for maximum fundamental frequency. *Comput. Struct. 86*, 2008.

[60] Ceyhan U Parnas L, Oral S. Optimum design of composite structures with curved fiber courses. *Compos Sci Technol*, 2003.

[61] Davis JE Nagendra S, Kodiyalam S. Optimization of tow fiber paths for composite design. *AIAA J*, 1995.

[62] A. Alhajahmad M.M. Abdalla Z. Gürdal. Design tailoring for pressure pillowing using tow-placed steered fibers. *J. Aircraft, 45(2)*, 2008.

[63] NASA. Integrated design tools reduce risk, cost. `http://spinoff.nasa.gov/Spinoff2011/t_2.html`.

[64] Phoenix Integration Inc., USA. *ModelCenter 11.0 Documentation*, 1998-2014.

[65] Tajima TMLH-101 – product data. `http://www.tajima.com`.

[66] Paul M. Weaver Ajit S. Panesar ., Kalyan Hazra. Investigation of thermally induced bistable behaviour for tow-steered laminates. *Composites: Part A 43*, 2012.

[67] Bingham CM Mellor PH Howe D Cossar C et al. Atallah K, Caparrelli F. Comparison of electrical drive technologies for aircraft flight control surface actuation. *Ninth international conference on electrical machines and drives.*, 1999.

[68] M.M. Abdalla A.W. Blom and Z. Gürdal. Optimization of course locations in fiber-placed panels for general fiber angle distributions. *CJ. Compos. Sc. Technol., 70(4)*, 2010.

[69] Z. Gürdal. Design of variable stiffness panels. *10th DOD/NASA/FAA Conference on Fibrous Composites in Structural Design, Vol. I*, 1994.

[70] Tatting B. F. *Analysis and Design of Variable Stiffness Composite Cylinders*. PhD thesis, Virginia Polytechnic Institute and State University, Blacksburg, VA, 1998. AIAA paper no. 1996-1569.

[71] Langley P. T. Finite element modeling of tow-placed variable-stiffness composite laminates. Master's thesis, Virginia Polytechnic Institute and State University, Blacksburg, VA, 1999.

[72] B. F. Tatting and Z. Gürdal. Analysis and design of variable stiffness composite cylinders. *13th U.S. National Congress of Applied Mechanics*, 1998.

[73] Akhavan H Ribeiro P. Natural modes of vibration of variable stiffness composite laminates with curvilinear fibers. *Compos Struct*, 2011.

[74] Akhavan H Ribeiro P. Non-linear vibrations of variable stiffness composite laminated plates. *Compos Struct*, 2012.

[75] Hallett SR Dang TD. A numerical study on impact and compression after impact behavior of variable angle tow laminates. *Compos Struct*, 2013.

[76] Lee HH. Hyer MW. The use of curvilinear fiber format to improve buckling resistance of composite plates with central circular holes. *Compos Struct*, 1991.